

Microcracks in New England granitoids: A record of thermoelastic relaxation during exhumation of intracontinental crust

Brett J. Nadan
Terry Engelder[†]

Department of Geosciences, The Pennsylvania State University, University Park, Pennsylvania 16827, USA

ABSTRACT

The upper intracontinental crust carries an excess horizontal compression, a remnant stress that arises because exhumation-related thermoelastic relaxation of deeper horizontal stress lags behind the reduction in overburden stress. This remnant stress appears in Earth stress data as an interchange in orientation of vertical σ_2 and horizontal σ_3 so that the ratio of least compressive horizontal stress (S_{hmin}) to vertical compressive stress (S_v) is >1 in much of the top 2 km of intracontinental crust. In theory, rocks exhumed from beneath 2 km should carry some record of this stress interchange, and this record is found in the orientation and density of healed, filled, and open microcracks in exhumed New England granitoids. Fluid inclusion planes (FIP) of older, healed microcracks are the best developed in a vertical orientation, and younger filled and open microcracks are best developed in the horizontal plane. Lateral unloading during initial isobaric cooling from the solidus of laterally constrained granite allows early microcrack growth once horizontal tension on the microscopic scale develops in response to vertical compression from the overburden load. During exhumation, further relaxation of lateral compressive stress takes place by a combination of decompression and cooling so that $\Delta S_{hmin}/\Delta S_v < 1$. Such behavior preserves a horizontal compression at depths < 2 km where horizontal microcracks are found. Excess horizontal compressive stress, a remnant of incomplete relaxation, carries upward right to the bedrock surface where near-surface structures such as stress-relief buckles and topographically related sheet fractures are found. This excess compression is consistent with the abundance of thrust fault focal mechanisms

found in the top 2 km of intracontinental crust east of the Rocky Mountain front and south of the U.S. border.

Keywords: granite, microcracks, exhumation, remnant stress, thermoelastic relaxation.

INTRODUCTION

Exhumation changes the state of stress within a body of rock, but near-surface stress-relief measurements show that exhumation never completely relieves horizontal stress as long as bedrock remains firmly attached (McGarr and Gay, 1978). As a general rule, exhumation leads to a state of near-surface horizontal compression even though the exposed bedrock surface is traction free (Hooker and Johnson, 1969; Ranalli and Chandler, 1975). This rule applies to both sedimentary and crystalline rocks (Engelder, 1984; Plumb et al., 1984). It is a near-surface horizontal compression that drives buckles on quarry floors following removal of overburden by excavation, an experiment in rapid exhumation (Adams, 1982). While postglacial buckles have been attributed to bending from glacial loading (Adams, 1989), near-surface horizontal compression is key to their formation as well. Near-surface compression generates a surface-normal tension and concomitant sheet fractures even when bedrock surfaces are tilted or curved (Holzhausen, 1989; Martel, 2006). Other structures in crystalline rocks attributed to the release of near-surface compressive stress include bornhardts (Twidale and Bourne, 1998), A-tents (or pop-ups) (Ericson and Olvmo, 2004), and displaced slabs (Twidale and Bourne, 2000). Horizontal compressive stress is such a broad phenomenon in near-surface processes that its origin merits further study.

In some instances, near-surface compressive stress is interpreted as residual arising from elastic stresses locked in the rock by forces balancing on either the microscopic

(Friedman, 1972; Voight and St. Pierre, 1974) or macroscopic scale (Coates, 1964; Voight, 1974). The problem with any residual stress model is that tensile stress should be present to counterbalance compressive stress in near-surface bedrock, and it is not found in the near surface (Engelder, 1993). This missing tensile stress suggests that some inelastic “buffering” process acts to maintain horizontal compression (McGarr and Gay, 1978). Mechanisms for stress buffering include swelling accompanying water adsorption (Harper, et al., 1979) and crack growth driven by internal stresses that produces large compressive changes in macroscopic stress (Bruner, 1979, 1984). Rather than pursuing a residual stress model reflecting a local equilibrium volume (Varnes and Lee, 1972) or a buffer-related model (Bruner, 1984), this paper examines conditions under which near-surface compressive stress is a manifestation of deep-seated lithostatic stress that has partially but not completely relaxed during exhumation. In this context, near-surface compression is a remnant stress in the sense that it is a deep-seated stress with a tectonic component that has survived exhumation-related thermoelastic relaxation (Voight, 1966; Engelder, 1993).

Attempts to understand the effect of exhumation on state of stress have assumed a crust that can support thermoelastic stresses (e.g., Price, 1966; Narr and Currie, 1982; Turcotte and Schubert, 2002). Exhumation-related horizontal stress arises under uniaxial strain conditions and includes two components that Turcotte and Schubert (2002) call the “thermal effect” and the “elastic effect [as a consequence of erosion]”. When acting independently, the former, here called *isobaric cooling*, leads to tension and is taken as the driving mechanism for joints during exhumation. Action of the latter during exhumation, here called *isothermal decompression*, may leave a component of horizontal compression in near-surface rocks depending on the pre-exhumation state of stress. Turcotte and Schubert (2002) state that

[†]E-mail: engelder@geosc.psu.edu

these two effects “are comparable for typical values of the geothermal gradient.” The purpose of this paper is to understand the origin of near-surface compressive stress by revisiting the question of whether Turcotte and Schubert’s (2002) two effects are comparable. The answer to this question is found in the interpretation of two data sets, one new and one published. The new data set encompasses the orientation and density of three types of microcracks in New England granitoids, and these data serve as a record of the evolution of thermoelastic stress during exhumation. The published set is a compilation of in situ stress data in the upper crust, and these data serve as a control to constrain our interpretation of exhumation-related thermoelastic stress based on microcrack data from New England granitoids.

BACKGROUND

Stress in Intracontinental Crust

The least compressive principal stress, σ_3 , is commonly horizontal in the middle portion of the brittle intracontinental crust but equally likely vertical in the upper kilometer or two (Fig. 1). This characteristic of the brittle crust is reflected in earthquake focal mechanism data from the eastern United States where strike-slip and normal fault mechanisms are indicative of horizontal σ_3 and thrust mechanisms indicate vertical σ_3 . Using the 58 focal mechanisms in the World Stress Map database from the USA east of longitude 104°W, strike-slip faulting is the most prominent mechanism at depths greater than 8 km, whereas thrust faulting is the most prominent mechanism at depths less than 8 km (Fig. 1). In particular, thrust and thrust-strike-slip mechanisms constitute 90% of all data in the top 2 km east of the Rocky Mountain Front. These focal mechanism data come from a region of North America where the maximum horizontal compressive stress, S_{Hmax} , is uniformly ENE. This depth-related change in focal mechanisms is akin to an interchange of the orientation of principal stress axes, σ_3 and σ_2 , in the shallow crust rather than a stress rotation.

The interchange of the orientation of principal stress axes, σ_3 and σ_2 , in the shallow crust appears in global compilations of stress measurements. An upwardly increasing ratio, R , of least horizontal to vertical stress ($R = S_{min}/S_v$ with compressive stress positive) is found within the top 2 km of the crust (Brown and Hoek, 1978). R continues to increase upward and becomes extreme within the zone of thermally and topographically induced compressive stress in the top few meters of the crust (Sbar et al., 1984; Martel, 2006). An upwardly increasing R

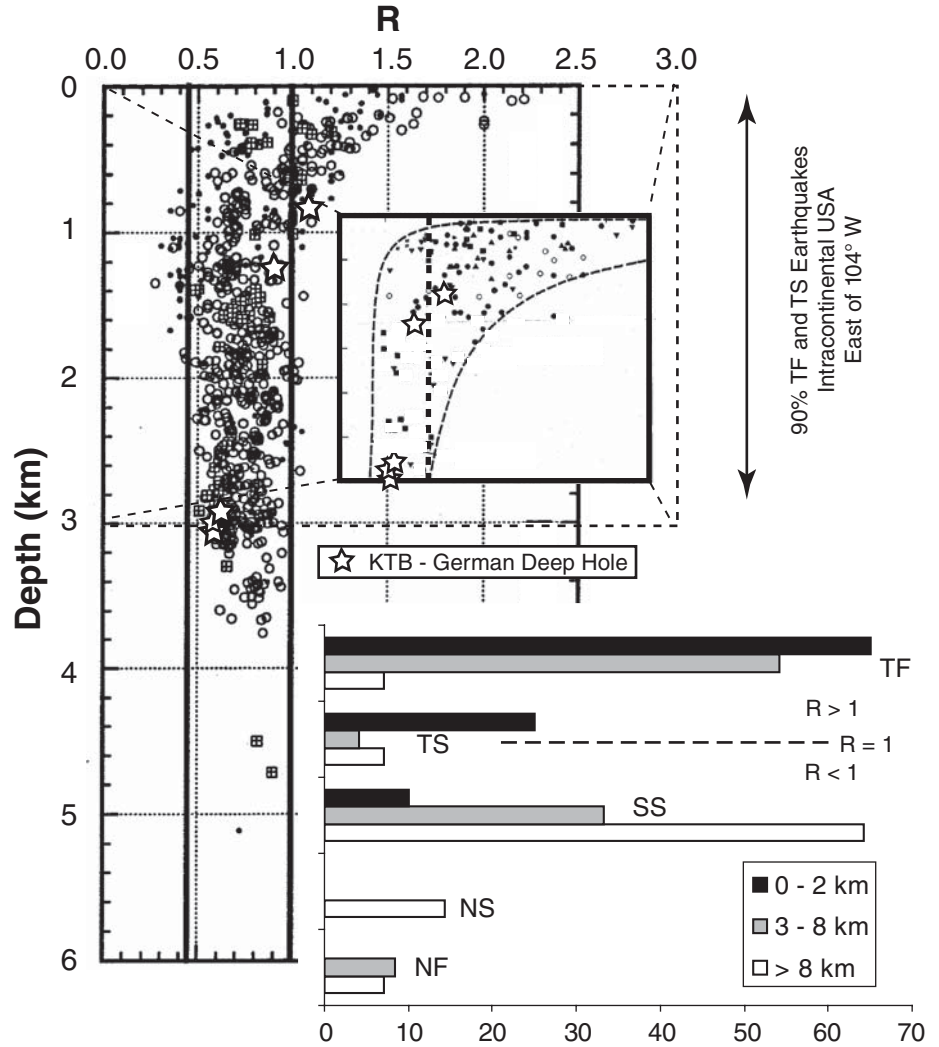


Figure 1. A Brown-Hoek stress profile (BHSP) to a depth of 6 km in sedimentary basins (adapted from Plumb, 1994). Data are categorized by lithology: sandstones (open circles), shales (filled circles), and carbonates (squares). Upper inset is an earlier BHSP including data from both crystalline and sedimentary rocks to a depth of 3 km where dashed line indicates $R = 1$ (adapted from Brown and Hoek, 1978). Data are categorized by continent: Scandinavia (open circle), Australia (solid circle), Canada (upright triangle), USA (overturned triangle), South Africa (square), and other regions (star). Lower inset shows a compilation of all 58 focal mechanisms from the United States east of longitude 104° (taken from the World Stress Map database). Data divided into three tiers as indicated. TF—thrust-fault mechanisms ($R > 1$), TS—thrust-strike slip mechanisms ($R \approx 1$), SS—strike-slip mechanisms ($R < 1$), NS—normal-strike-slip mechanisms ($R < 1$), NF—normal fault mechanisms ($R < 1$).

is characteristic of sedimentary basins including regions of normal faulting (Plumb, 1994) and in crystalline basement such as the Bohemian massif, Germany (Brudy et al., 1997), thus indicating that the causal mechanism for the interchange of the orientation of principal stresses (i.e., σ_2 and σ_3) is not an artifact of sedimentary rocks. Looking downward into the crust, the trend of $R < 1$ continues into crystalline basement to depths of at least 8.6 km, the deepest in situ stress mea-

surement to date (Brudy et al., 1997; Lund and Zoback, 1999). The same trend carries downward through a combination of sedimentary cover over crystalline basement as seen in the Great Lakes region of North America (Haimson and Doe, 1983). The stress profile showing an increase in R upward through the shallow crust is referred to as the *Brown-Hoek stress profile* (BHSP) in honor of its discoverers (Brown and Hoek, 1978). In this paper we make the case that

the BHSP is a manifestation of an exhumation-related remnant stress.

Total stress in the crust reflects a superposition of components, some of which may be eliminated in searching for the mechanism responsible for the BHSP. First, vertical stress ($S_v = g\rho_{ob}z$), a function of integrated overburden density, ρ_{ob} , gravity, g , and depth, z , is nearly linear with depth in the upper crust except in the near surface in regions of topographic relief where horizontal compressive stress is high (e.g., Miller and Dunne, 1996; Martel, 2006). Because the upward increase in R starts below depths affected by topographic relief, the BHSP must reflect a mechanism that carries horizontal compressive stress, S_{hmin} , into the top 2 km of the crust. The limits of horizontal stress in the upper crust are governed by frictional strength along fault zones (Byerlee, 1978). Such strength along normal and thrust faults provides lower and upper bounds for the BHSP in an actively deforming Earth (Zoback and Townend, 2001). However, frictional strength is overburden dependent so that friction-related stress is linear with depth and goes to zero in the near surface (Zoback, 2007). Friction does not offer a mechanism for the interchange of the orientation of σ_2 and σ_3 in the shallow crust (e.g., Brace and Kolstedt, 1980).

While stress measurements within some Plio-Pleistocene sedimentary basins come from rocks that are being buried for the first time and, hence, are still subject to consolidation (Karig and Hou, 1992), the majority of stress measurements come from either crystalline rocks (Herget, 1993) or sedimentary rocks where lithification terminates consolidation (Plumb, 1994). Many of these older rocks are partially unloaded as a consequence of exhumation as is the case for the western end of the Bohemian massif and the larger North America platform. Unloading takes place with the removal of overburden and its concomitant decrease in vertical stress (i.e., $-\Delta S_v$). Partial or complete exhumation causes a decrease in S_{hmin} as well (i.e., $-\Delta S_{hmin}$). For a shallow crust consistent with the BHSP, $\Delta S_{hmin}/\Delta S_v < 1$, and this is also the condition necessary for an interchange of the orientation of σ_2 and σ_3 when σ_3 is horizontal in the deep crust. The guiding axiom of this paper is that such an interchange of σ_2 and σ_3 is the manifestation of thermoelastic relaxation as rocks are gradually exhumed (Price, 1966; Voight and St. Pierre, 1974; Haxby and Turcotte, 1976). In this context, thermoelastic relaxation is the response of the horizontal compressive stress (i.e., $-\Delta S_{hmin}$) to a decrease in both vertical stress, $-\Delta S_v$, and temperature, where

$$\frac{\Delta S_{hmin}}{\Delta S_v} < 1. \quad (1)$$

Microcracks

In addition to those that may have propagated under a high-stress anisotropy usually through the superposition of a tectonic stress, microcracks are a product of thermoelastic relaxation (e.g., Nur and Simmons, 1970; Plumb et al., 1984; Fleischmann, 1990; Jang and Wang, 1991; Vollbrecht et al., 1991; Wise, 2005). In granite, quartz hosts both intragranular and transgranular microcracks (Kranz, 1983). These are of three general types: open, filled with a foreign mineral, and healed with crystallographically continuous quartz that leaves fluid inclusion "planes" (FIP). The thesis of this paper is that the differences in orientation and density among FIP, filled microcracks, and open microcracks in quartz grains reflect the evolution of earth stress accompanying thermoelastic relaxation during exhumation. It is an exhumation-related thermoelastic relaxation that leads to the BHSP, to a unique distribution of intracontinental focal mechanisms, and to the formation of near-surface structures such as sheet fractures, bornhardts, A-tents (or pop-ups), and displaced slabs.

Vertical microcracks commonly constitute a fabric in the upper crust as indicated by data from 200 granite and granite-gneiss quarries in New England (Dale, 1923). Two dominant strikes of vertical microcracks (i.e., NS and EW) are observed throughout much of New England (Wise, 1964). Other regions hosting a regional fabric of vertical and subvertical microcracks include the Piedmont of Virginia (Tuttle, 1949), the Massif Central of France (Lespinasse and Pecher, 1986; Pecher et al., 1985), the Oshima granite of Japan (Takemura et al., 2003), and the Beartooth uplift of Montana (Wise, 2005). Such a fabric is seen along core from wells drilled in Illinois (Kowallis et al., 1987), the Rhine Graben of France (Dezayes et al., 2000), and Japan (Takeshita and Yagi, 2001).

A particularly important, but commonly overlooked aspect to the regional microcrack fabric in granites is the pervasive occurrence of horizontal microcracks as indicated by the orientation of the rift plane (i.e., the quarry direction of easiest splitting) in granitoids of New England (Dale, 1923). The rift plane is horizontal in 96% of the granite quarries from Merrimack Synclinorium as reported by Dale (1923), while 21% of the granites west of the Bronson Hill anticlinorium in Vermont have a horizontal rift (Fig. 2). Farther to the northwest in the Canadian Shield, rift is predominantly horizontal in Precambrian granites (Osborne, 1935).

The orientation of rift is easily detected by means of an anisotropy in rock properties that arises from open microcracks rather than to either FIP or filled microcracks (Friedman and

Bur, 1974). For example, Barre granite of Vermont displays its lowest modulus in the horizontal direction normal to a vertical rift plane, whereas the Stanstead and Laurentian granites from the Canadian shield display their lowest modulus in the vertical direction normal to a horizontal rift (Douglass and Voight, 1969). Despite the presence of a horizontal rift in the two Canadian granites, FIP are best developed in the vertical orientation (Douglass and Voight, 1969), thus indicating the absence of a temporal link between FIP and open microcracks.

DATA GATHERING

To refine our understanding of the BHSP as manifest by microcracks in the granites of New England, we collected samples from over 40 quarries and outcrops throughout New England. From these, we chose six specimens, one from outcrop and five from quarries examined by Dale (1923) in Massachusetts, New Hampshire, and Vermont (Fig. 2). Three of the five quarries were the subject of an earlier study of sheet fractures in New England granite (i.e., Jahns, 1943; Johnson, 1970). The granites include Pennsylvanian (Milford—two specimens), Devonian of Neo-Acadian age (Concord and Barre), and Devonian of Acadian age (Bethlehem [from an outcrop] and Chelmsford) (Robinson et al., 1998; Bradley et al., 2000). The three younger granites have a uniform texture and lack a distinct foliation, whereas the two Acadian granites have coarse biotite and muscovite (as large as 5 mm) and are foliated, the Bethlehem more strongly so although not to the extent that it would be described as a gneiss, per se. Among the five, only the Milford (a quartz syenite at 19% quartz) falls just outside the modal composition for granite.

Except for the Chelmsford granite, samples from the quarries were oriented relative to the mutually perpendicular directions used to excavate the rock (Fig. 3). In the language of the quarryman, the *rift* is the plane of easiest splitting, and the *hardway* is the plane of greatest resistance to splitting with the *grain* falling between the extremes in terms of ease of splitting (Wise, 1964; Johnson, 1970; Engelder, 1993). In New England, the hardway is generally vertical, whereas the rift or grain may be horizontal depending on the region (Dale, 1923). Quarries in the Chelmsford, Concord, and Milford granites have a horizontal rift, whereas the quarries in the Barre granite have a vertical rift (Fig. 2).

Three oriented and mutually perpendicular thin sections of each sample were prepared for flat-stage and U-stage analysis under the polarizing microscope. Our focus was on quartz grains that, as elastic bodies, are scale-independent, and

as such, act like spherical, solid-inclusion stress-meters, however irregular (Engelder, 1993). Our analysis was limited to quartz because feldspar commonly splits along cleavage planes, thus yielding a false impression of the true orientation of the controlling stress field (Kranz, 1983). In addition to the relatively isotropic behavior of quartz with regard to crack propagation, its relatively low birefringence and optical relief allow easy identification of various types of cracks. Furthermore, the thermal expansion coefficient, α , of quartz is more than three times larger than feldspar (Skinner, 1966), allowing thermal stresses to accumulation at a faster rate per ΔT than feldspar when laterally confined. In each thin section, crack orientations, crack types, crack density, and grain size were recorded in ten or eleven of the largest quartz grains (≈ 1 mm). We examined only the largest quartz grains on the presumption that microcracking was more likely to reflect larger scale stress fields rather than microscopic stress concentrations. However, the irregular shape of microcracking suggests that even in the larger grains, the regional stress field was modified by the irregular shape of the host grain (Fig. 4).

Our microcrack data were collected on a flat stage without the benefit of image analysis techniques (e.g., Lespinasse et al., 2005) for a couple of reasons. First, manual inspection assured that all microcracks were correctly identified by type. Second, flat-stage data allowed for a more effective visual display of microcrack orientation distribution than the more quantitative stereonet projection. In ten or eleven of the largest quartz grains in each of three mutually perpendicular thin sections, all microcracks were identified and strikes measured. Crack density was measured in the same grains using a method described by Wilson et al. (2003). Because we were most interested in crack density cutting three mutually perpendicular planes and not spacing, we did not apply the cosine correction necessary for spacing analyses. The microcrack density was determined by counting the number of microcracks that intersected scan lines measuring 3 mm, 0.75 mm, or 0.375 mm, depending on the size of the grain. Shorter scan lines (i.e., 0.75 mm and 0.375 mm) were used on smaller grains, such as those in the syntectonically recrystallized Chelmsford granite. Within each grain, three scan line directions were identified using a random number generator, and a count of all microcracks was performed in each direction with the scan line running through the same point near the center of the grain. The number of microcracks intersected by the scan line is divided by the length of the line to obtain a density measurement in units of cracks per unit length (mm). The data were then averaged for the 10–11 quartz grains in each thin section.

MICROCRACK ORIENTATION AND DENSITY

Although microcracks within the quartz grains of New England granites are slightly curved to complex in thin section, their surface may be represented by a plane with different operators agreeing on a manual best-fit to within a few degrees (Fig. 4). Fluid inclusion planes (FIP) are just as complexly curved and irregular as open microcracks, leaving little doubt that the latter was the progenitor of the former. The open microcracks are of two varieties: single, isolated discontinuities that are slightly curved to complexly curved, and networks of cracks that are most apparent at high magnification (Fig. 4D). Networks are particularly well developed in horizontal rift planes of the Bethlehem, Concord,

and Milford granites. A third type of microcrack, filled microcracks, constitutes a small minority of the total population (i.e., between 0% in the Barre granite and 7% in the Bethlehem granite) with the filling mineral(s) having a high birefringence. A compilation of manually fit planes to microcracks serves to define the fabric in specimens of New England granite.

Concord Granite

To depict microcrack development in New England granite, the fabric of the Neo-Acadian Concord granite serves as the standard against which the fabric of others is compared. The Concord was sampled in the Swenson quarry of the Swenson Granite Company, Concord, New Hampshire. During the early twentieth

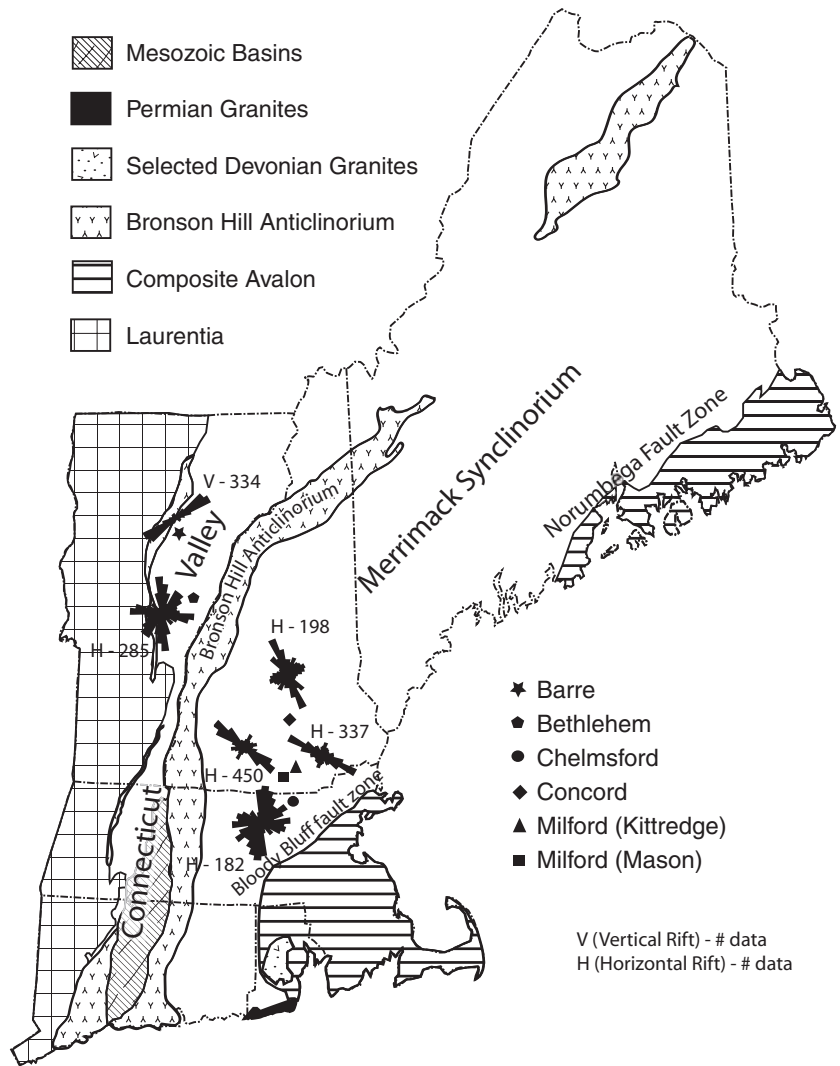


Figure 2. Simplified geological map of New England showing sample locations and the strike of all microcracks in the horizontal thin sections. FIP are the dominant microcrack.



Grain Wall
Flame Cut

272 data

474 data

Hardway Wall
Wire Saw

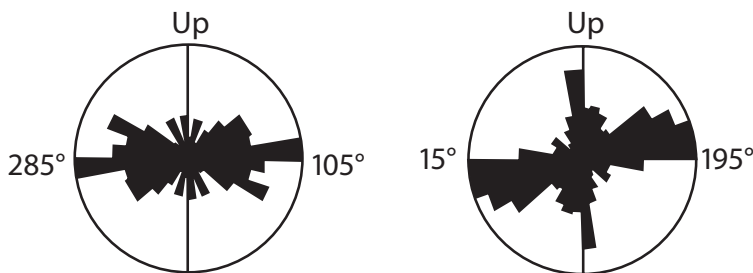


Figure 3. The Milford granite at the Mason quarry, Milford, New Hampshire. The view is to the east with a rough, flame-cut wall to the left (i.e., the grain wall) and a smooth, wire-sawed wall to the right (the hardway wall). Rose diagrams show microcrack distribution of all microcracks as seen in vertical thin sections cut parallel to the grain and hardway walls. The horizontal microcrack population is responsible for the horizontal rift in this quarry.

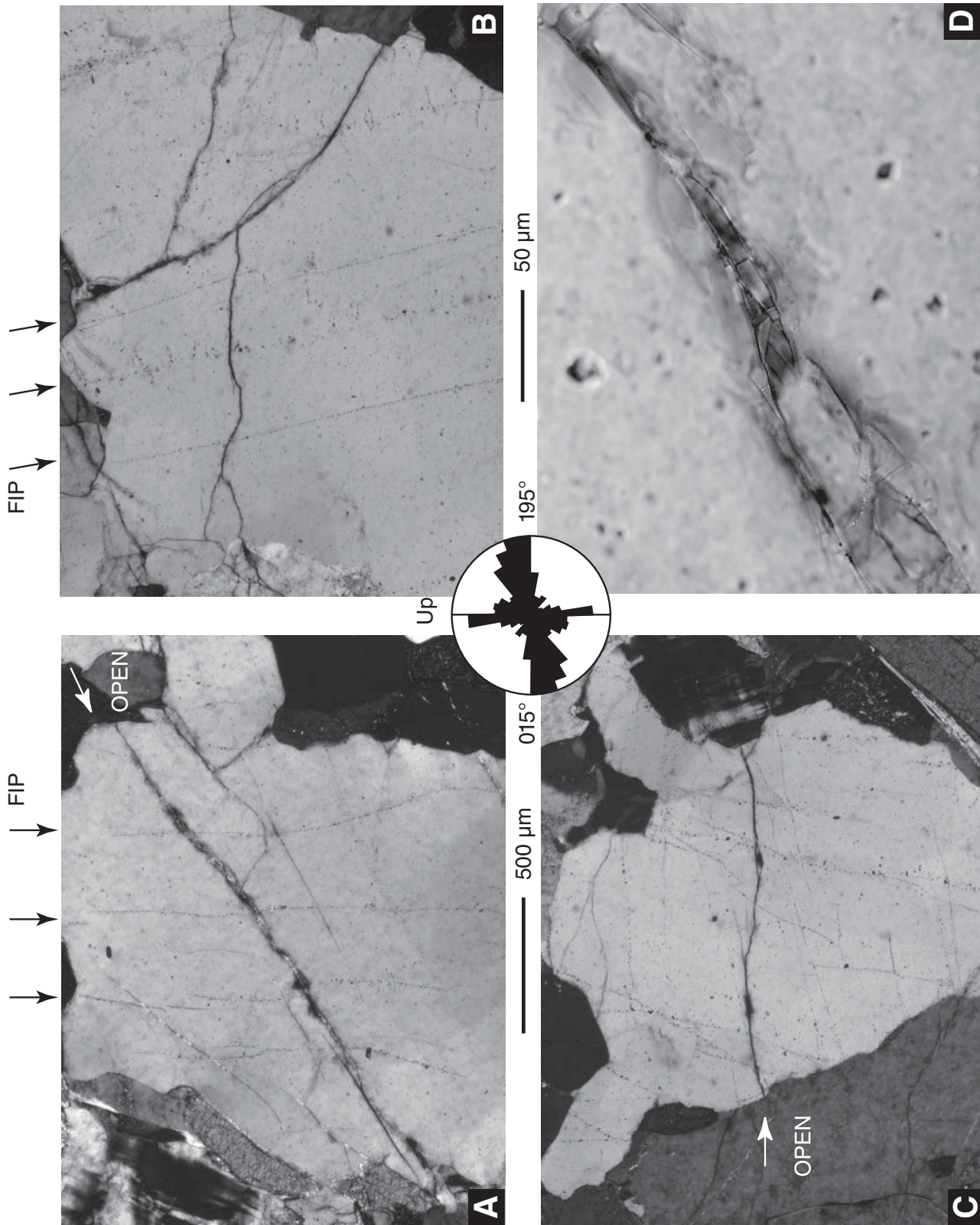


Figure 4. (A)–(C) Samples of Milford granite from the Mason quarry, Milford, New Hampshire. Thin sections of quartz grains cut in the vertical orientation parallel to the hardway wall of the Mason quarry (crossed nicols). Inset shows a rose diagram of all microcracks (474 data) measured in quartz grains cut parallel to the hardway (refer back to Fig. 3 for a view of the Mason quarry). Each thin section is oriented in the same manner as the rose diagram so that FIP are the common vertical microcrack and open cracks are the common horizontal microcrack. (D) Example of open networks of microcracks in the Barre granite, Barre, Vermont. These are rift cracks in a thin section cut parallel to the hardway.

century, the Concord granite district consisted of six quarries, all with sheet fractures that are either subhorizontal or dipping gently but with dip directions that differed by as much as 180° (Dale, 1923). During early operations, grain walls were cut between N40°E and N90°E (Dale, 1923), whereas the modern Swenson quarry cuts its grain wall to the SE.

Quartz grains within the Concord granite contain the three types of microcracks mentioned above. The orientation fabric and relative density of each type is illustrated using a sample cube and an orthographic projection of the three faces of that sample cube (Fig. 5). Often the best view of a microcrack fabric is normal to the quarry hardway for the simple reason that microcracks of both the rift and grain planes are seen in cross section (Fig. 4). Looking normal to the hardway, the FIP are best developed vertically with a strike of ~330°, which is slightly off from the direction of the quarry's grain wall. A secondary set of FIP appears in the rift (horizontal) plane as seen in both vertical (i.e., hardway and grain) sections. The origin of the tilt of both the primary and secondary set of FIP to the NE, as seen normal to the hardway plane, does not correlate with the west-dipping sheet fractures of the Swenson quarry (Dale, 1923). Healed and open microcracks are best developed on the rift (horizontal) plane as seen in both vertical thin sections. The "horizontal" microcracks have a slight tilt in the same direction as the FIP normal to the quarry hardway. Because all the microcracks in each quartz grain were tabulated, it is readily apparent that the density of FIP far exceeds that of the open microcracks which, in turn, exceeds the density of filled microcracks. These observations apply to other granites where FIP are more common than open microcracks. Likewise, there is a preferred growth of open microcracks in the horizontal plane versus a preferred growth of FIP in the vertical orientation.

Milford Granite (Mason Quarry)

Two active quarries, both operated by the Fletcher Granite Company, are presently found in the Milford granite district south of Milford, New Hampshire—the Mason and the Kittredge. A century ago, the district had as many as 15 active quarries (Dale, 1923). The topographic grain, if any, is roughly NS over the Milford district. The dip direction of sheet fractures among these 15 early quarries is variable, but more quarries carry sheets dipping normal to the NS grain of the topography (Dale, 1923). In the Milford granite, several grain walls were cut in directions between N80°W and N65°W through roughly horizontal sheet fractures (Fig. 3).

Microcracks in quartz grains of the Pennsylvanian Milford granite, sampled in the Mason quarry, constitute a fabric similar to that within the Concord granite (Fig. 6). In this case, the vertical FIP appear most prominently when looking normal to the rift (horizontal) plane, whereas the less common open microcracks are best developed in the horizontal plane as seen looking normal to the hardway. Filled microcracks only appeared in the vertical orientation and are thus combined with open microcracks. Horizontal FIP are less well developed than in the Concord granite but have about the same density as horizontal open microcracks. Vertical open cracks are less common yet, and scatter as is typical for a view normal to one preferred orientation of microcracks.

Chelmsford Granite

The Acadian Chelmsford granite was sampled in the Fletcher quarry at Chelmsford, Massachusetts. There, sheet fractures are subhorizontal (Johnson, 1970). As quarry development progressed, grain walls (i.e., direction of the flame cut) were gradually adjusted from N25°E to N40°E (Fig. 7).

Quartz grains in the Acadian Chelmsford granite, sampled in the Fletcher quarry at Chelmsford, Massachusetts, are syntectonically recrystallized and <1 mm across (versus 2–3 mm for other plutons of this study). Consequently, the counts of microcracks are lower because less cross sectional area was sampled in 10–11 grains per thin section. Nevertheless, the microcrack fabric in the Chelmsford is similar to that of the Concord and Milford granites with FIP prominently developed in the vertical orientation and open microcracks prominently developed along the quarry rift (i.e., the horizontal orientation) (Fig. 7). FIP are best developed in the NS direction and seem to have no bearing on the orientation of the quarry grain wall. The change in orientation of the grain wall (direction of the wire saw) with time is consistent with the search for a weak fabric within the collection of open, vertical microcracks.

Bethlehem Granite

The one outcrop sample of this study is the Acadian Bethlehem granite, which displays a foliation of biotite dipping at 45° toward the SSE. Sheet fractures are poorly developed in this outcrop at the Grantham rest stop on Interstate 89, Vermont. The Bethlehem granite carries the same microcrack fabric as the three previous granites and thus shows a vertical FIP and horizontal open microcracks (Fig. 8). An additional set of vertical FIP have grown nor-

mal to the most prominent set. Filled and open microcracks in the vertical orientation show little tendency to cluster in a preferred orientation. Subhorizontal filled and open microcracks show a tendency to dip in the opposite direction from the foliation (Fig. 8). Based on the microcrack fabric, one might predict that a quarry in the Bethlehem granite would also be characterized by a horizontal rift.

Milford Granite (Kittredge Quarry)

In the Kittredge quarry of the Milford granite, the grain walls cut N85°W with the dip direction of the sheet fractures toward 105° (Fig. 9). While the grain and hardway directions in the Kittredge quarry are nearly identical in strike to those in the Mason quarry, microcrack development is somewhat anomalous. The grain plane is characterized by open microcracks in addition to the more common FIP (Fig. 9). This quarry also has a set of horizontal FIP and a secondary set of vertical FIP. Horizontal microcracks define the quarry rift, although the excavation of many blocks benefit from the presence of sheet fractures.

Barre Granite

Barre granite district, Barre, Vermont, is characterized by topographic domes with long axes striking about N25°E and interspersed valleys of the same trend. The distribution of sheet fractures in active quarries in the early twentieth century is consistent with topographic trends with the majority of sheets dipping either NW or SE (Fig. 10C). The Barre granite differs from granites to the SE in New England by having a vertical rift plane (Dale, 1923). During quarry operations in the Barre granite, rift walls were cut anywhere from N28°E to N65°E (Fig. 10D).

In the Barre granite, sampled at the Pierre-Adams quarry (Rock of Ages), quartz grains have a single vertical FIP set (Figs. 10A and 10B). The microcrack fabric in the Barre resembles its counterpart in the Kittredge quarry by having two well-developed open microcrack sets including a horizontal set and a vertical set striking in the direction of the quarry rift. Unlike the Kittredge quarry, the vertical open microcracks are consistent with a vertical rift.

Microcrack Density

A quantitative expression of fabric development is reflected in crack density data from these six samples of Paleozoic (i.e., #/mm) (Table 1). In terms of thin section orientation, the most densely developed microcracks are vertical FIP as seen in horizontal thin sections. Horizontal FIP are less dense. The most densely developed

Concord Granite (Swenson Quarry)

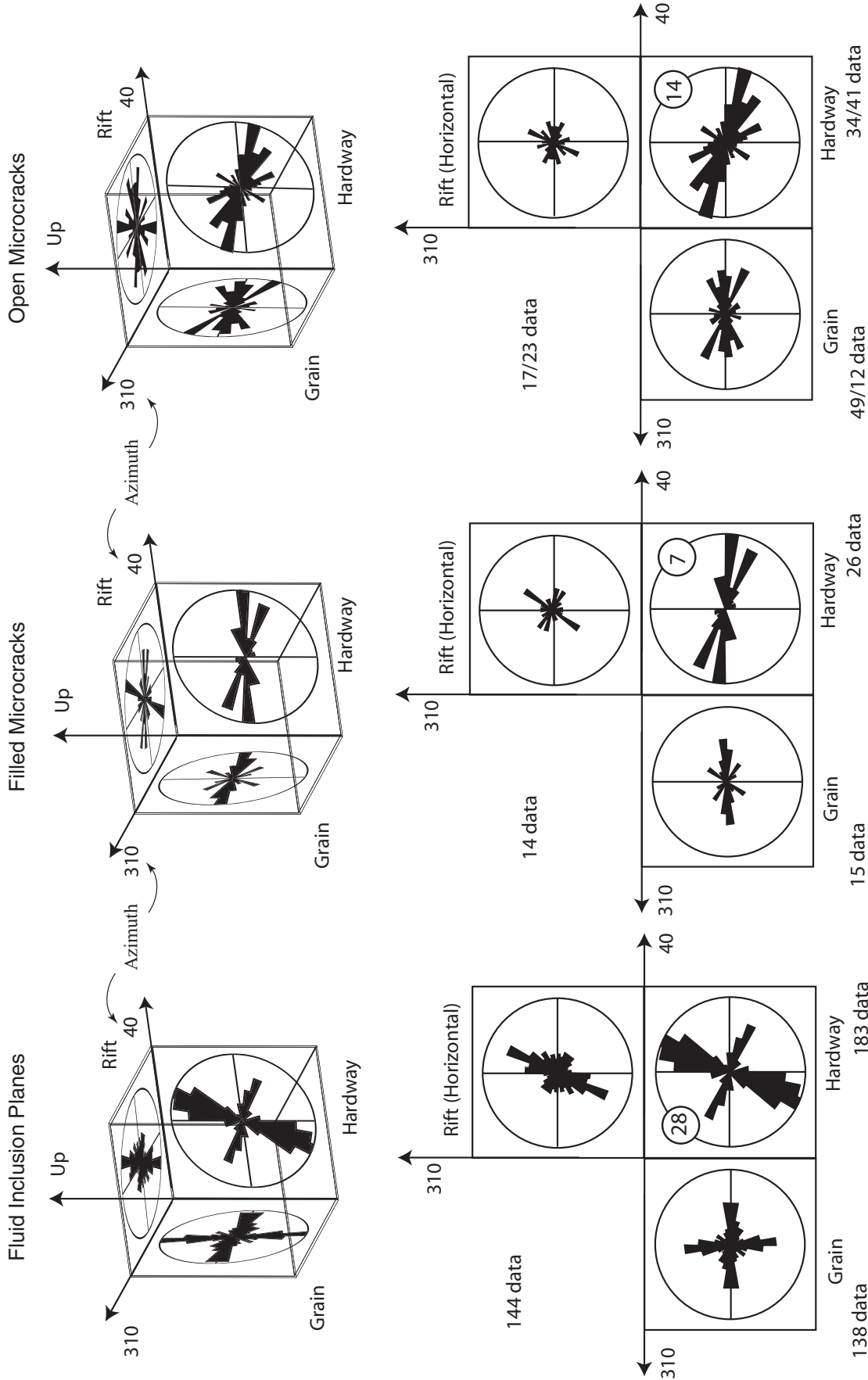


Figure 5. Fabric of microcracks within quartz grains of the Concord granite (Swenson quarry) near Concord, New Hampshire. Orientation data displayed in the form of rose diagrams for microcracks measured in a thin section cut in the orientation indicated by azimuthal arrows. Orientation data are binned into 10° intervals. First row: Data cube with microcrack orientations presented in the form of three mutually perpendicular rose diagrams. Labels on the faces of the data cube indicate planes in the working quarry known as rift (horizontal), grain, and hardway. Second row: Orthographic projection of the three sides of the microcrack data cube. Mutually perpendicular data are scaled so that the outer ring has a data count indicated by the circled number. Each type of microcrack has a different maximum data count. The data count for the open microcracks includes (open networks)/(open single microcracks).

Milford Granite (Mason Quarry)

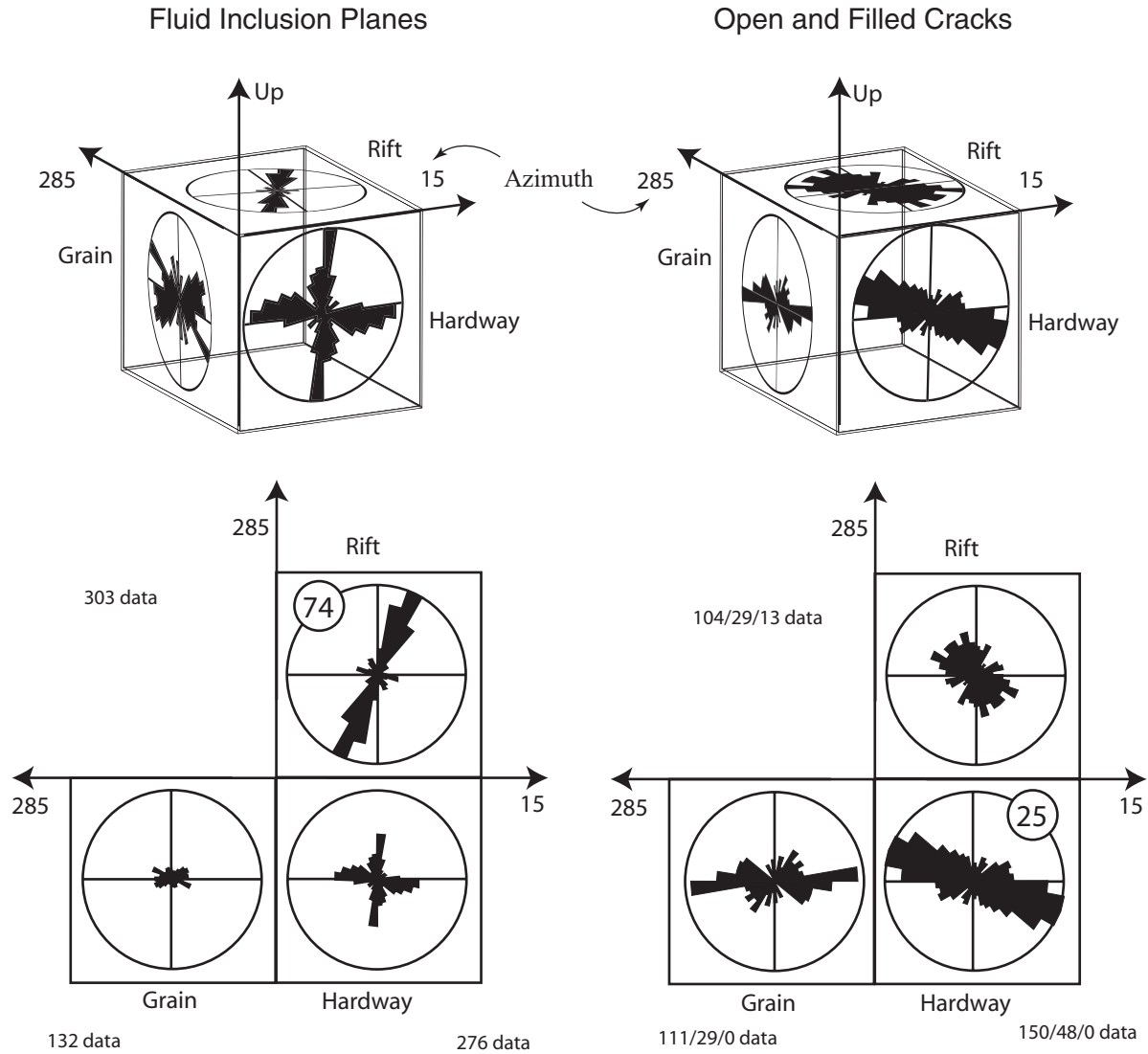


Figure 6. Fabric of microcracks within Milford granite (Mason quarry) southwest of Milford, New Hampshire. See Figure 5 caption for further explanation. Note: Working directions in the Mason quarry follow Dale's original designation and are so labeled.

Chelmsford Granite (Fletcher Quarry)

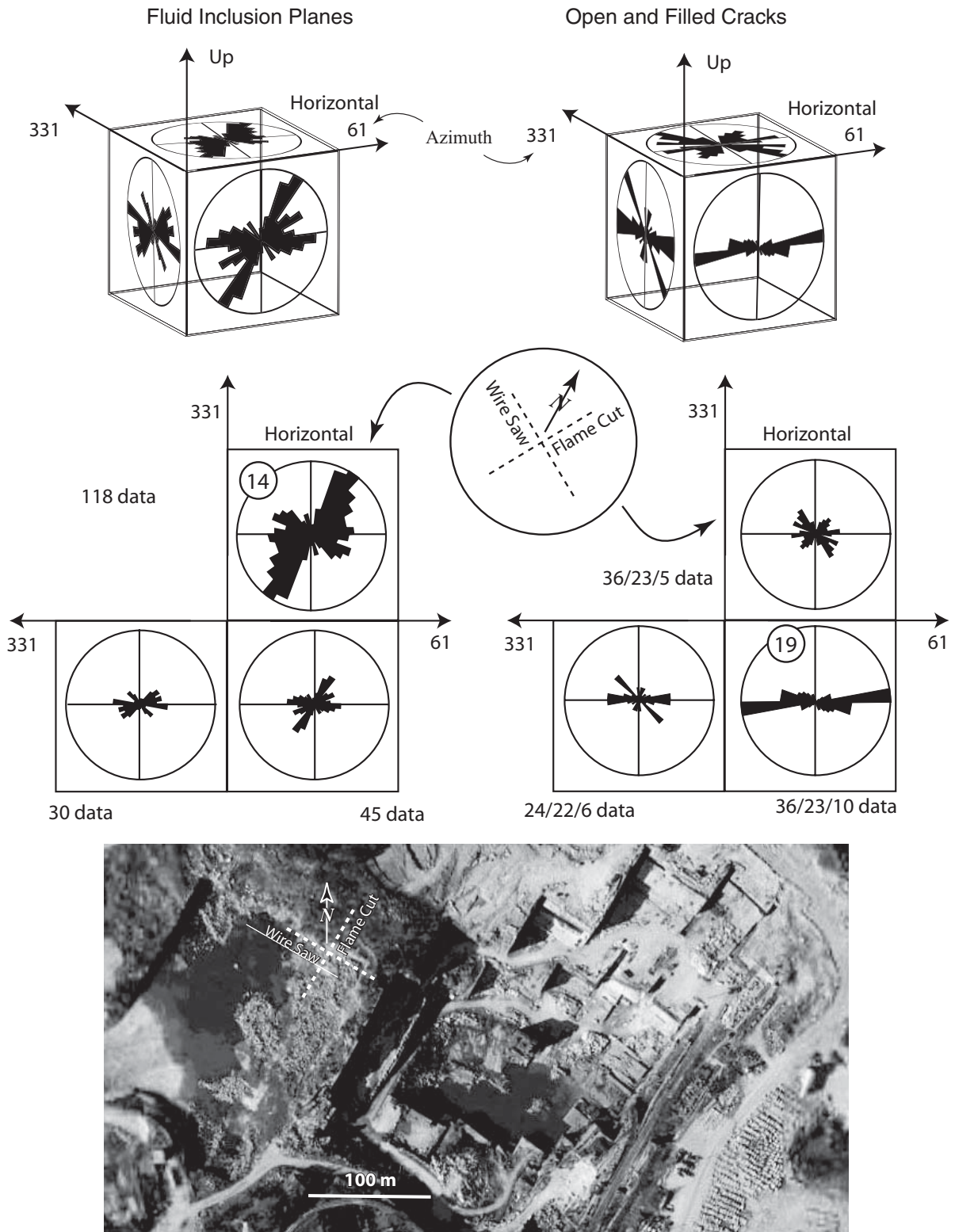


Figure 7. Fabric of microcracks within Chelmsford granite (Fletcher quarry) near Chelmsford, Massachusetts. Three orthogonal thin sections cut along arbitrary directions of azimuth 331° , 061° , and horizontal. See Figure 5 caption for additional explanation. Note: Working directions in the Fletcher quarry are called flame cut, wire saw, and horizontal. Google Earth image of the Fletcher quarry shows the clockwise rotation of the directions in the working quarry from the older portions (west) to the newer portions (east).

Bethlehem Granite (Grantham Rest Stop I-89)

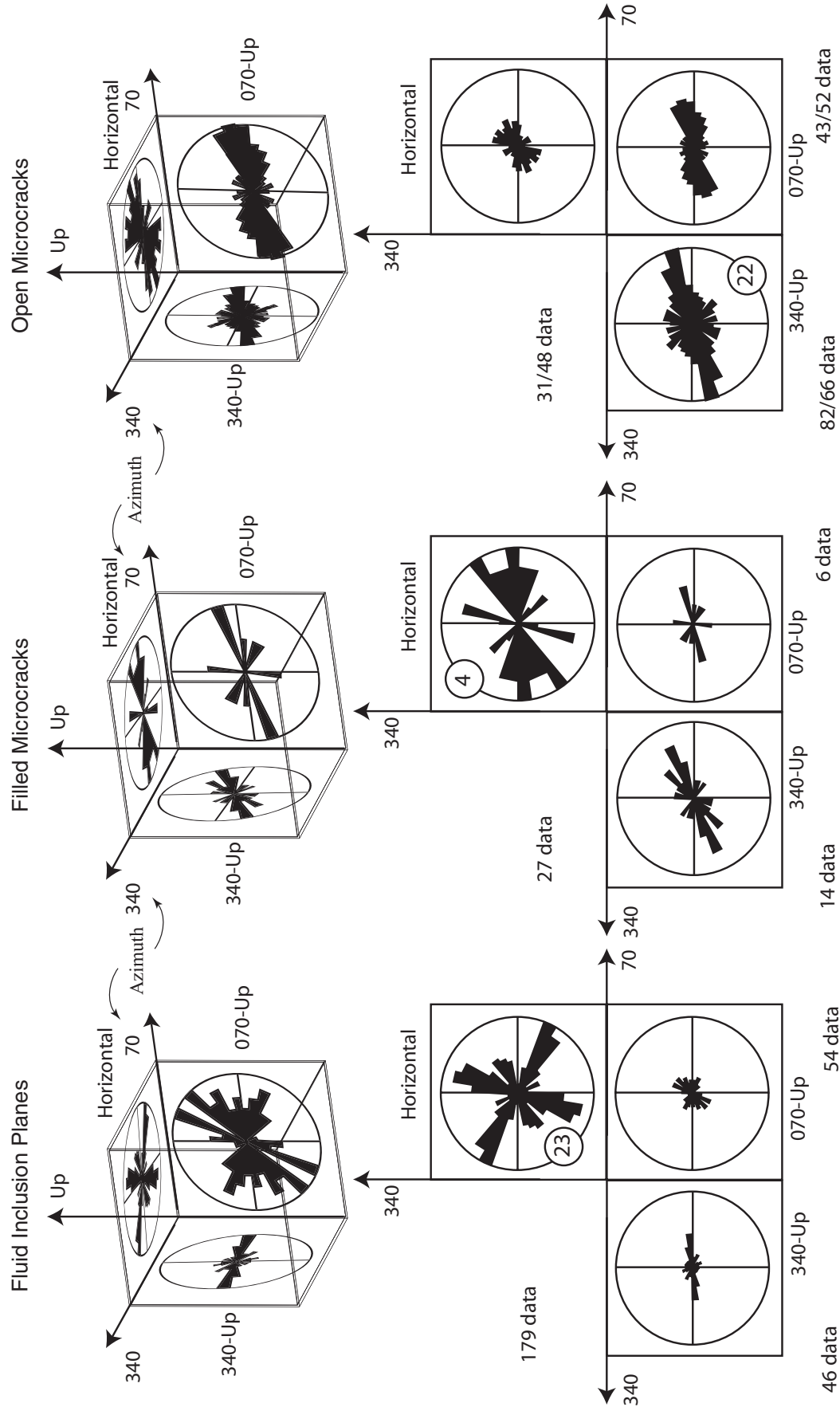


Figure 8. Fabric of microcracks within the Bethlehem granite (outcrop) near Grantham, Vermont. See Figure 5 caption for further explanation. Because this sample comes from an outcrop where quarry directions have not been established, labels on the faces of the data cube are outcrop orientations with no connection to rift, grain, or hardway.

Milford Granite (Kittredge Quarry)

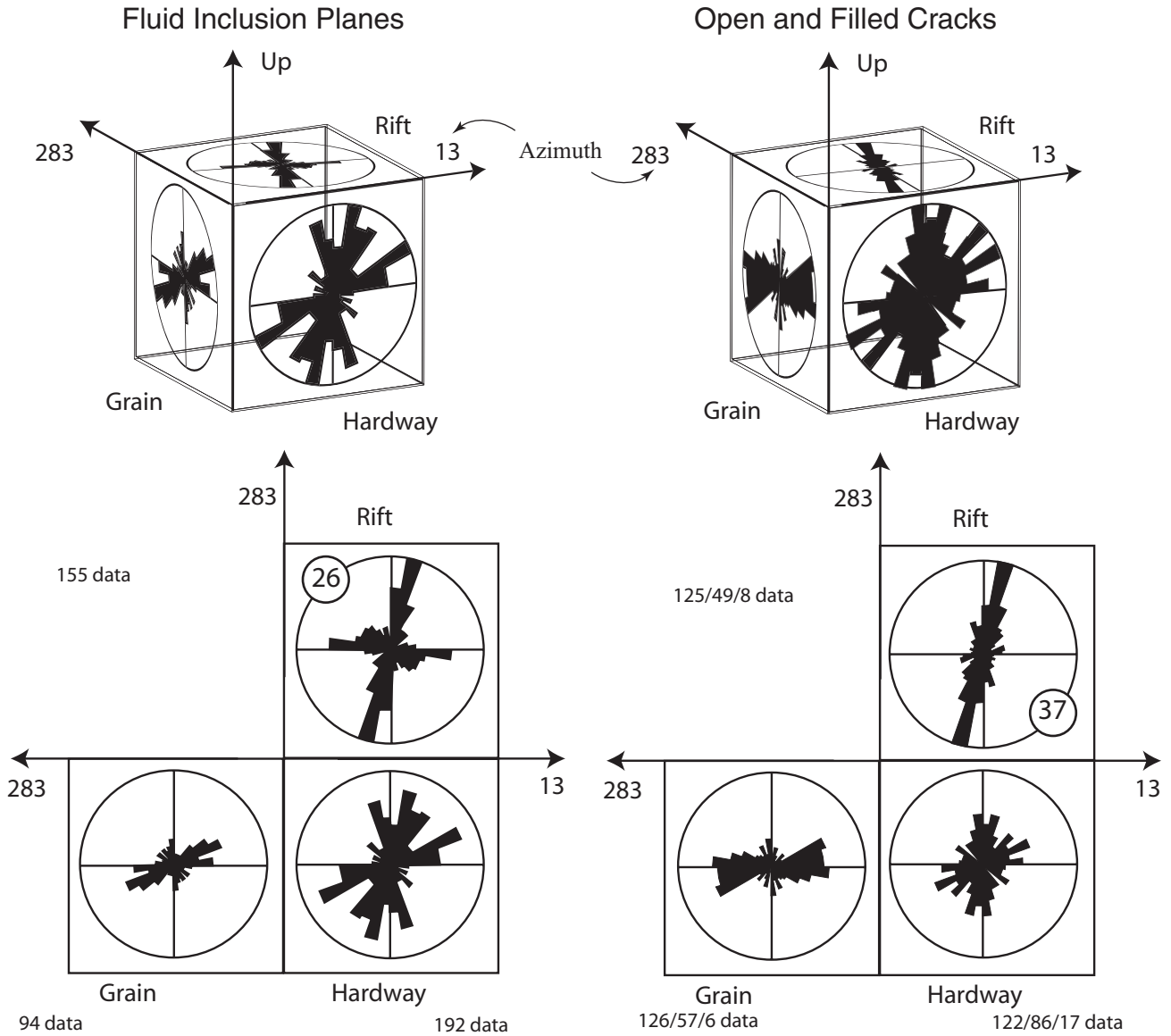


Figure 9. Fabric of microcracks within the Milford Granite (Kittredge quarry) in Milford, New Hampshire. See Figure 5 caption for further explanation. Labels on the faces of the data cube indicate planes in the working quarry known as grain (horizontal), rift, and hardway.

TABLE 1. SUMMARY OF CRACK DENSITIES IN NEW ENGLAND GRANITES		
Horizontal thin sections	Fluid inclusion planes	Open cracks
	Crack density (#/mm)	Crack density (#/mm)
Barre (grain)	1.33 ± 0.6	0.98 ± 0.6
Bethlehem (rift)	1.29 ± 0.8	0.65 ± 0.3
Chelmsford (rift)	1.64 ± 1.0	0.67 ± 1.0
Concord (rift)	1.87 ± 1.4	0.36 ± 0.4
Milford (Kittledge) (rift)	0.89 ± 0.6	1.29 ± 0.8
Milford (Mason) (rift)	2.18 ± 0.8	1.2 ± 0.9
Average	1.53 ± 0.5	0.86 ± 0.4
Vertical thin sections		
Barre (hardway-rift)	1.32 ± 0.4	0.85 ± 0.4
Bethlehem (70°–340°)	0.56 ± 0.3	1.40 ± 0.6
Chelmsford (hardway-grain)	0.56 ± 0.4	1.09 ± 0.7
Concord (hardway-grain)	1.38 ± 0.6	1.11 ± 0.6
Milford (Kittledge) (hardway-grain)	1.91 ± 0.8	1.85 ± 0.7
Milford (Mason) (hardway-grain)	1.65 ± 0.7	1.76 ± 1.7
Average	1.23 ± 0.4	1.34 ± 0.6

Barre Granite (Pierre-Adams Quarry)

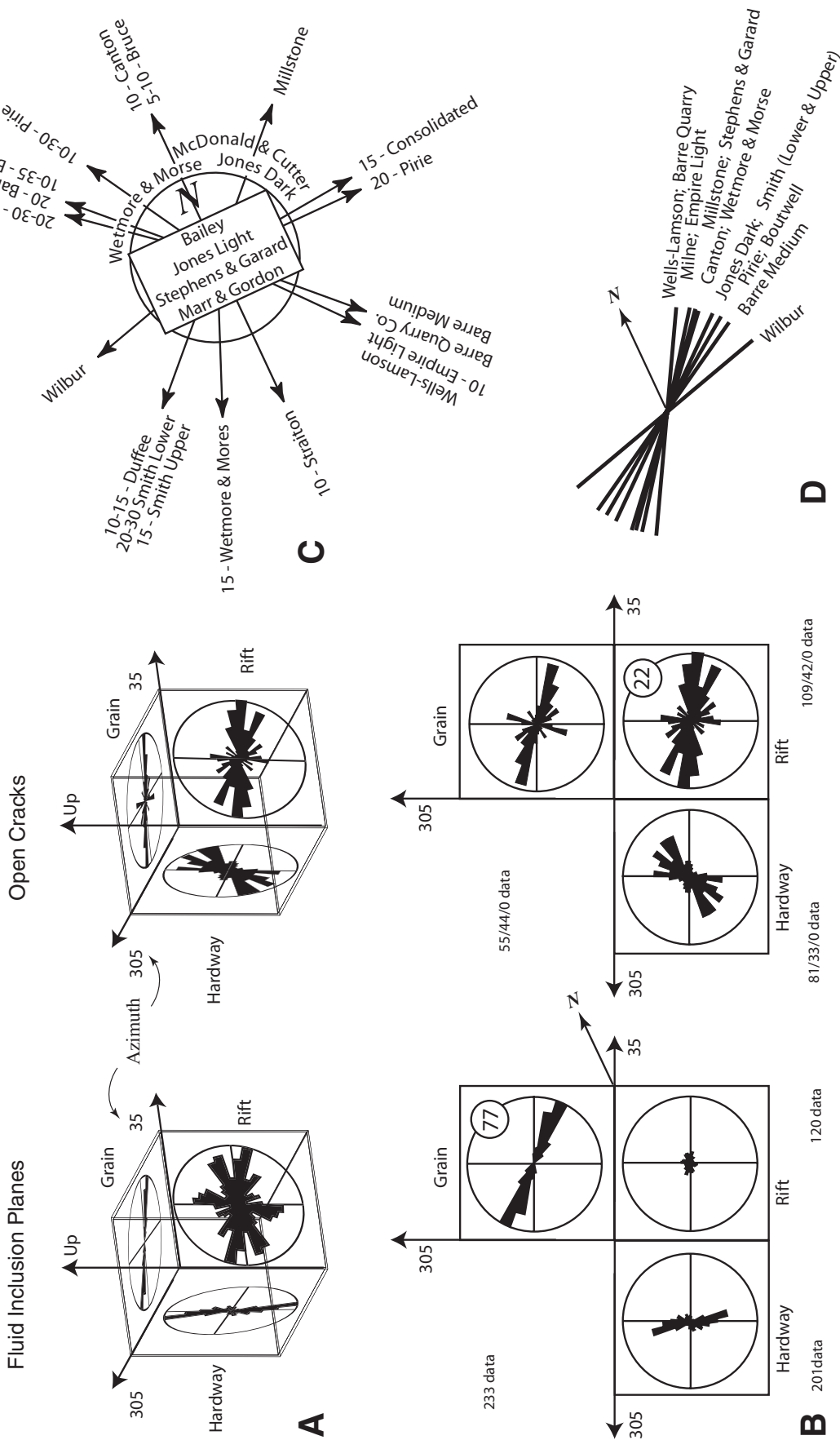


Figure 10. Fabric of microcracks within the Barre granite (Pierre quarry) near Barre, Vermont. See Figure 5 caption for further explanation to parts (A) and (B). Labels on the faces of the data cube indicate planes in the working quarry known as grain (horizontal), rift, and hardway. (C) Dip and dip directions for 19 quarries in Barre granite (Dale, 1923). Three quarries have horizontal sheet fractures, and four quarries (box) are without well-developed sheet fractures. (D) Directions of vertical rift planes in 14 quarries in Barre granite (Dale, 1923).

open microcracks are horizontal as seen in vertical thin sections. In vertical thin sections, it is seen that FIP are predominantly vertical cracks (Fig. 4). These numbers confirm the qualitative observations using sample cubes (Figs. 5–10).

DISCUSSION

The paragenetic sequence for microcracking in the Paleozoic granite of New England starts with cracks that subsequently heal with crystallographically contiguous quartz (i.e., FIP), includes cracks that are filled with a foreign mineral, and ends with open cracks. Photomicrographs provide independent evidence witnessing the same sequence of microcrack growth (Fig. 4). First, the open microcracks cut the FIPs. Second, the FIPs could not have propagated across open microcracks. If the FIPs propagated away from the open microcracks, one would not expect aligned FIPs on both sides of microcracks. The same arguments follow for filled microcracks that cut the FIP. Open microcracks crosscut filled microcracks, whereas filled microcracks would not have propagated across open microcracks. If two open microcracks crosscut simultaneously and then filled, they should have filled simultaneously. Thus the sequence of microcracking reflects the paragenesis of healing first, then filling, and finally the propagation of open microcracks. Because healing is most rapid under hot (i.e., deep) conditions and is slow to nonexistent at $T < 200$ °C (Smith and Evans, 1984), this paragenesis of microcracks witnesses a horizontal σ_3 when the granite was deep and a vertical σ_3 after exhumation carried the granite to shallow levels of the crust. Such an interchange in orientation of σ_3 is consistent with an upper brittle crust characterized by the BHSP.

Other studies of microcracking in granite report the same paragenetic sequence starting with vertical FIP and ending with open, horizontal microcracks (e.g., Lespinasse and Pecher, 1986; Laubach, 1989). Within the Mesozoic granites of New England, FIP have been interpreted as propagating during “post-emplacement cooling,” whereas open microcracks develop during “exhumation by re-cracking (vertical) healed fluid inclusion planes” (i.e., Fleischmann, 1990). Vertical FIP and open, horizontal microcracks are found in the Blanco Perla granite of Spain (Durucan et al., 2000). The same relative density of vertical FIP and horizontal microcracks is documented in the Oshima granite, Japan (Takemura et al., 2003). Even when the rift is vertical or not well developed, as is the case for other Japanese granites (and the Barre granite), the horizontal plane carries open microcracks (Chen et al., 1999). The granites of the western

Bohemian massif, Germany, contain vertical FIP that are interpreted as consequence of “thermal cracking” at crustal levels >5 km, whereas open, horizontal microcracks form at <5 km where “tectonic and gravitational stresses” are key (Vollbrecht et al., 1991). We will make the case that while the driving stress for open, horizontal microcracks (S_{Hmax}) may have a tectonic component, it is the exhumation-related preservation of the horizontal stresses in the form of remnant stresses that leads to an interchange of σ_2 and σ_3 and gives rise to the BHSP.

There is a tendency for the growth of a modest number of horizontal FIP in each granite with the exception of Barre. Like the focal mechanisms from the eastern USA, which indicate some spatial variation in R between 8 and 3 km (Fig. 1), the FIP suggest a temporal variation in R . The simplest explanation is that exhumation carried the granite into the upper regime of $R > 1$ before temperatures cooled to the point that microcrack healing ceased, the temperature for which may be as low as 85 °C (i.e., Laubach, 1989). Another explanation might involve the superposition of a component of tectonic shortening that would drive the interchange of stress principal at a deeper crustal level than seen in the BHSP.

The Stress that Drives Microcracks

Microcracks are a manifestation of absolute tension on the microscopic scale even when the host granite is subject to the large compression found several km below the Earth’s surface. One candidate for driving microcracks is the tensile stress arising from mismatches between the thermoelastic properties of minerals within granite (Nur and Simmons, 1970; Savage, 1978; Bruner, 1984). Thermoelastic stresses are generated when grains lock together and act as lateral constraints on nearest neighbors during either a temperature change or a stress change or some combination of the two. Because the coefficient of thermal expansion of quartz exceeds that of feldspar, cooling of granite will lead to tensile stress in the quartz. Calculations involving an idealized granite show that a 300 °C temperature drop generates a change in stress, $\Delta\sigma = -480$ MPa in quartz, a stress sufficient to negate the effect of overburden compression and trigger crack propagation from all but the smallest of flaws in a quartz grain (Savage, 1978). An equally impressive suite of microcracks is produced by stress relief (i.e., decompression) upon removal of a core from depth, a consequence of the mismatch of elastic properties among locked grains (Carlson and Wang, 1986).

If thermoelastic mismatches on the microscopic scale operate without the superposition of body forces like gravity and other mecha-

nisms for generating a stress anisotropy, microcracking in adjacent quartz grains of isotropic grain orientation are unlikely to assume a preferred orientation. A microcrack fabric is the product of the superposition of an overburden stress and/or tectonic stress upon thermoelastic stress (Jang and Wang, 1991). An axially symmetric anisotropy may be generated without the help of a tectonic stress, if thermoelastic relaxation takes place within a laterally constrained granite body (Narr and Currie, 1984). The FIP in New England granite develop a vertical fabric because of the presence of a post-solidus tectonic stress during cooling through the solidus. Here, tectonic stress arises through any process that causes a stress anisotropy in the horizontal plane (i.e., $S_{Hmax} > S_{Hmin}$) (Engelder, 1993). When granite is subject to a significant stress anisotropy, several mechanisms are likely responsible for the generation of microcracks including wedging grain boundaries, sliding along planes of weakness, elastic mismatches, and pore crushing (Wong, 1982; Hazzard et al., 2000). However, it may be a mistake to think that either the vertical FIP or horizontal microcracks within New England granites were “driven” by tectonic stress, per se.

Vertical Microcracks

Aside from the usual mechanisms for microcrack generation under a stress anisotropy, another possibility for the generation of early, vertical microcracks is axial loading across vertical grain diameters (Fig. 11A). Compression in the form of a vertical load, F_v , across the vertical diameter can produce a horizontal tension within an unsupported short cylinder (Hondros, 1959). This suggests the possibility that, under the right conditions, quartz grains would develop vertical opening mode cracks, parallel to the gravitational body force. While it is a stretch to argue that the shape and interlocking of quartz in granite are natural examples of unsupported cylinders, the concept is worthy. In this model, thermoelastic relaxation of horizontal stress serves only to relieve the lateral constraint but not generate the tensile stress. As long as lateral stress is compressive, however small, problems such as buckling of a stack of grains do not arise (Fig. 11A).

The analytical solution for the distribution of stress within a solid cylinder is as follows (Hondros, 1959). Assume a vertical force, F_v , is applied on a line contact with the side of a cylinder of radius, r , and length, l . F_v is calculated by taking S_v and multiplying that by the cross-sectional area A of the cylinders, such that $A = 2lr$. The horizontal stress, σ_h , at the central point on the vertical diameter of a cylinder laying on its side is

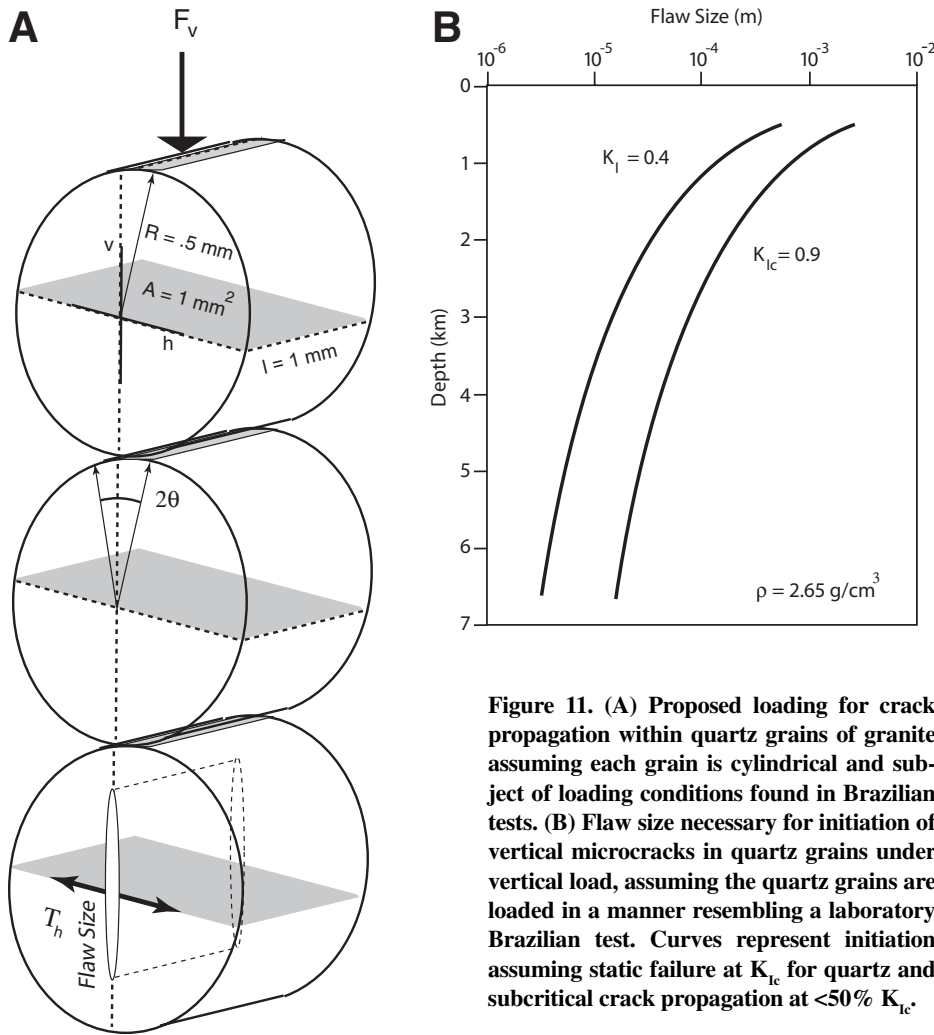


Figure 11. (A) Proposed loading for crack propagation within quartz grains of granite assuming each grain is cylindrical and subject of loading conditions found in Brazilian tests. (B) Flaw size necessary for initiation of vertical microcracks in quartz grains under vertical load, assuming the quartz grains are loaded in a manner resembling a laboratory Brazilian test. Curves represent initiation assuming static failure at K_{Ic} for quartz and subcritical crack propagation at $<50\% K_{Ic}$.

$$\sigma_h = -\frac{F_v}{\pi lr} \quad (2)$$

The same analysis holds to an error of 4% for a flattened Brazilian disc as long as the contact angle, θ , is greater than a value, $2\theta > 20^\circ$ (Wang et al., 2004).

From Equation 2, the internal tension is proportional to the vertical load, but it is not immediately obvious that this internal tension will drive microcracks. The size of a “Griffith” flaw necessary for microcrack propagation within quartz grains is given by

$$c = \left(\frac{K_{Ic}}{Y\sigma_h} \right)^2, \quad (3)$$

where K_{Ic} is the fracture toughness of quartz, Y is the shape factor (arbitrarily set to 1), and c is the half length of the flaw (Lawn, 1993). Despite the large vertical load for granite

under 6 km of overburden, for example, fracture toughness of quartz (i.e., 0.9 MPa-m^{1/2}) requires initial “Griffith” flaws of nearly 100 μ m, which are not apparent in the quartz grains of granite (Fig. 11B). However, cracks may propagate from smaller flaws under subcritical conditions (e.g., Martin, 1972). If, for example, propagation takes place under subcritical conditions where $K_I = 0.4$ MPa-m^{1/2}, then flaws on the order of 10 μ m may serve to initiate microcrack propagation.

The appeal of this model is that microscopic tensile stress within quartz grains are generated without the necessity of a net tension transmitted across the entire granite body. A net tension across the entire granite body would inevitably produce large vertical joints, something not seen in quarries such as the Mason (Fig. 3). The long-term uniaxial compressive strength of granite is greater than 100 MPa and much more when slightly confined (Eberhardt et al., 1999; Szczepanik et al., 2003). With its strength

and a modest lateral confinement, granite will sustain the weight of overburden without collapsing under shear failure to depths approaching 8 km. However, at loads of about half their ultimate strength in laboratory tests, granite samples develop incipient microcracks (Brace et al., 1966). This accounts for growth of vertical microcracks in plutons cooling from the solidus. While tectonic stress generates a modest stress anisotropy in the horizontal plane, the responsible stress for crack propagation is vertical and comes from the large anisotropy developed between the vertical direction and horizontal plane.

Evolution of Stress in Granite

One of the most reliable rules for crack propagation is that cracks align normal to σ_3 during propagation and will curve during growth to find this preferred orientation (Pollard and Segall, 1987). From this rule, we know that early, deep microcrack propagation in granite took place where σ_3 was horizontal and late, shallow microcrack propagation took place where σ_3 was vertical. Aside from our argument involving microcrack paragenesis, a qualitative mechanical argument pointing to deeper propagation normal to a horizontal σ_3 comes from the spacing of FIPs. The traces of very closely spaced FIPs (“close” means the distance between the FIPs is small relative to their trace lengths) is diagnostic of the driving stress being small relative to the difference between the ambient principal stresses (Olson and Pollard, 1989). The ambient stress at the time the FIPs formed must have been highly anisotropic. A large stress anisotropy is characteristic of propagation at great depth where overburden stress (S_v) remains constant and high while horizontal stress is reduced by cooling.

A second general rule for crack propagation is that the driving stress comes from one of two general sources: absolute tension and internal fluid pressure (Pollard and Aydin, 1988; Bergbauer and Martel, 1999). Some have argued that super-hydrostatic fluid pressure is the primary driving stress for initial microcrack propagation in granite (Takeshita and Yagi, 2001). If this were so, fluid inclusions in quartz grains should have trapping pressures and temperatures at conditions found near the solidus of post-tectonic granites. Yet, the earliest fluid inclusions generally have trapping temperatures more than 100 °C below the solidus (i.e., Jang and Wang, 1991).

Small fluid-filled cavities trapped within quartz of granite undoubtedly serve as one flaw type capable of triggering initial microcrack propagation in subsolidus quartz. While fluids within the cavities could even lend a compo-

ment to crack driving stress, they are not interconnected and have no mechanism for self-generating the higher fluid pressure required of hydraulic fracture. Rapid cooling relieves fluid pressure in inclusions and moves the host quartz grains away from a state favoring decrepitation of primordial fluid inclusions. For this reason, tension from gravitational loading (i.e., Equation 2), requires thermoelastic relaxation in a laterally constrained body before initiation of post-solidus microcracking, particularly the FIPs. Such relaxation occurs after a temperature drop of more than 100 °C below the solidus (Jang and Wang, 1991; Vollbrecht et al., 1991).

Lithostatic Stress

Because magma has relatively low shear strength under static conditions, tectonic stress rapidly dissipates and granites solidify from magmas under a stress state close to lithostatic stress, if not exactly lithostatic, S_L , with

$$S_L = S_v = S_{Hmax} = S_{Hmin}, \quad (4)$$

where equal principal stresses include S_v , the vertical compressive stress, plus S_{Hmax} and S_{Hmin} , the greatest and least horizontal compressive stresses (Engelder, 1993). Hence, the initial stress state in subsolidus granite is lithostatic or nearly so. This is, perhaps, an example where horizontal stresses are largely a consequence of the weight of overburden. Starting at the solidus

of granite, thermoelastic relaxation modifies the lithostatic stress state giving rise to successive stress states consistent with the BHSP depending on relative rates of cooling and exhumation (Price, 1979; Vollbrecht et al., 1991). When acting separately, *isobaric cooling* and *isothermal decompression* induce markedly different stress paths (Fig. 12). Isobaric cooling takes place when overburden thickness does not change as the pluton cools and is commonly accepted as the mechanism giving rise to columnar joints (DeGraff and Aydin, 1987). Isothermal decompression takes place during removal of overburden under constant temperature, a rare condition outside of the explosive injection of kimberlite pipes. The question is how do these two stress paths each lead to microcrack growth during the thermoelastic relaxation of granite.

Isobaric Cooling

For a laterally constrained, isotropic material, the lateral normal stress change ΔS_{Hmin} corresponding to a temperature change ΔT is

$$\Delta S_{Hmin} = \frac{\alpha_t E}{1 - \nu} \Delta T \quad (5)$$

(Haxby and Turcotte, 1976). For intact granite, the Young’s modulus is $E = 16\text{--}70$ GPa (Haas, 1989), Poisson’s ratio is $\nu = 0.15$ (Birch, 1966), and the coefficient of thermal expansion is $\alpha_t =$

$8 \times 10^{-6} \text{ } ^\circ\text{C}^{-1}$ (Skinner, 1966). With these thermoelastic properties, the thermoelastic relaxation occurs at a rate between -15 MPa and -66 MPa per $100 \text{ } ^\circ\text{C}$ decrease. Microcracking is expected where the thermal stress change overcomes the sum of the material tensile strength, σ_t , (Nasseri et al., 2005) and the compressive lithostatic stress, S_L , such that

$$\left| \frac{\alpha_t E}{1 - \nu} \Delta T \right| > |\sigma_t| + S_L. \quad (6)$$

Using the typical thermoelastic properties (i.e., $E = 70$ GPa) and $S_v = S_L = 159$ MPa (assuming $z \approx 6$ km with an overburden density of 2.65 g/cm^3), a $-\Delta T$ of $235 \text{ } ^\circ\text{C}$ is required to completely negate the initial lithostatic stress after cooling through the solidus. This estimate of temperature drop is larger for granite with a lower E or higher ν . Of course, microcracking is possible long before the lithostatic stress is completely negated. Fluid inclusions in the healed microcracks suggest that crack healing began at temperatures of $\sim 400 \text{ } ^\circ\text{C}$ and that it was complete at $\sim 200 \text{ } ^\circ\text{C}$ assuming a relatively simple cooling history for Precambrian granite of the Illinois basin (Kowallis et al., 1987). In this case, healed microcracks are not found at higher temperatures because $\Delta T > 200 \text{ } ^\circ\text{C}$ is required for microcrack initiation. This is consistent with a cap of $\sim 400 \text{ } ^\circ\text{C}$ for trapping temperature of

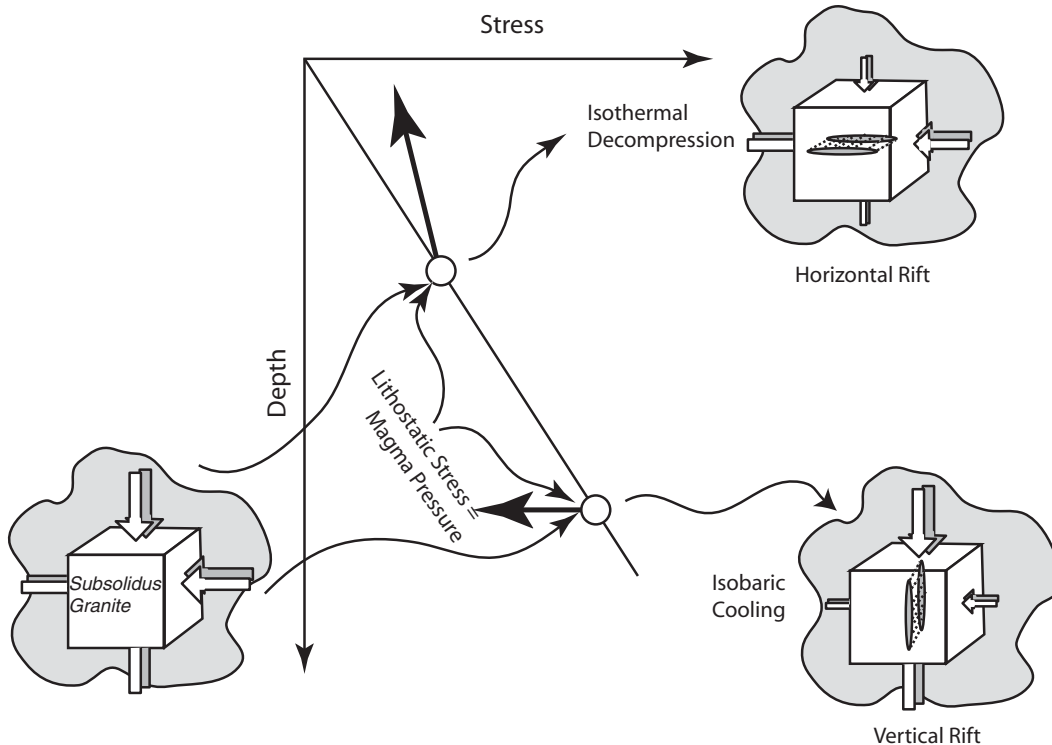


Figure 12. Stress-depth curve showing the lithostatic stress. Dark arrows are stress paths for isothermal decompression and isobaric cooling. Three cubes are hypothetical models of stress in granite for lithostatic stress at the solidus, after isobaric cooling, and after isothermal decompression. Double arrows on the cubes show the relative magnitudes of the horizontal and vertical principal stresses.

fluid inclusions in post-tectonic granite of New England (Winslow et al., 1994). Finally, isobaric cooling sets up a state of stress consistent with the deep portion of the BHSP as horizontal stress decreases without a change in the vertical stress while generating a stress anisotropy favoring microcracking prior to the development of pluton-wide absolute tension. The fabric in FIP indicates the presence of a tectonic stress that is responsible for $S_{Hmax} > S_{hmin}$.

Decompression and the BHSP

Isobaric cooling takes granite to a state of stress where $S_{hmin} < S_v$, a state common in the brittle crust below a depth of 2 km (Brown and Hoek, 1978; Plumb, 1994). This is the starting point for exhumation driven thermoelastic relaxation, which reflects components of both decompression and cooling. Taken separately, isothermal decompression is the sum of the horizontal compressive stress change developed during the removal of laterally confined overburden

$$\Delta^ob S_{hmin} = \frac{\nu}{1-\nu} \Delta S_v \quad (7)$$

and the compressive stress change induced by a change in radius of isostatically compensated exhumed crust

$$\Delta^r S_{hmin} = \frac{E}{(1-\nu)} \frac{\rho_c}{\rho_m} \frac{\Delta z}{a}, \quad (8)$$

where Δz is negative when a thickness of the crust removed by erosion, a is the radius of the Earth after erosion, ρ_c is the density of the crust, and ρ_m is the density of the mantle (Haxby and Turcotte, 1976). An early analysis pointed out that exhumation-related decompression could lead to a large excess horizontal compressive stress (Voight, 1966).

To achieve a stress state consistent with the interchange of the orientation of σ_2 and σ_3 and the BHSP, the following condition must be met: the rate of thermoelastic relaxation (i.e., $\Delta S_{hmin}/\Delta z$), which also includes the effect of cooling along a geothermal gradient, must be a fraction of the overburden gradient so that

$$\frac{\Delta S_{hmin}}{\Delta z} = \frac{\Delta^r S_{hmin} + \Delta^ob S_{hmin} + \Delta^t S_{hmin}}{\Delta z} < \frac{\Delta S_v}{\Delta z}, \quad (9)$$

where Δz is negative during exhumation. No tectonic term is present in Equation 9 so that $S_{hmin} = S_{Hmax}$. Equation 9 means that $\Delta S_{hmin}/\Delta S_v < 1$ during exhumation.

Although we conclude that $\Delta S_{hmin}/\Delta S_v < 1$ for the development of the BHSP, we first need to define the range of $\Delta S_{hmin}/\Delta S_v (= R^*)$ that allows a thermoelastic relaxation consistent with the BHSP starting at some initial stress representa-

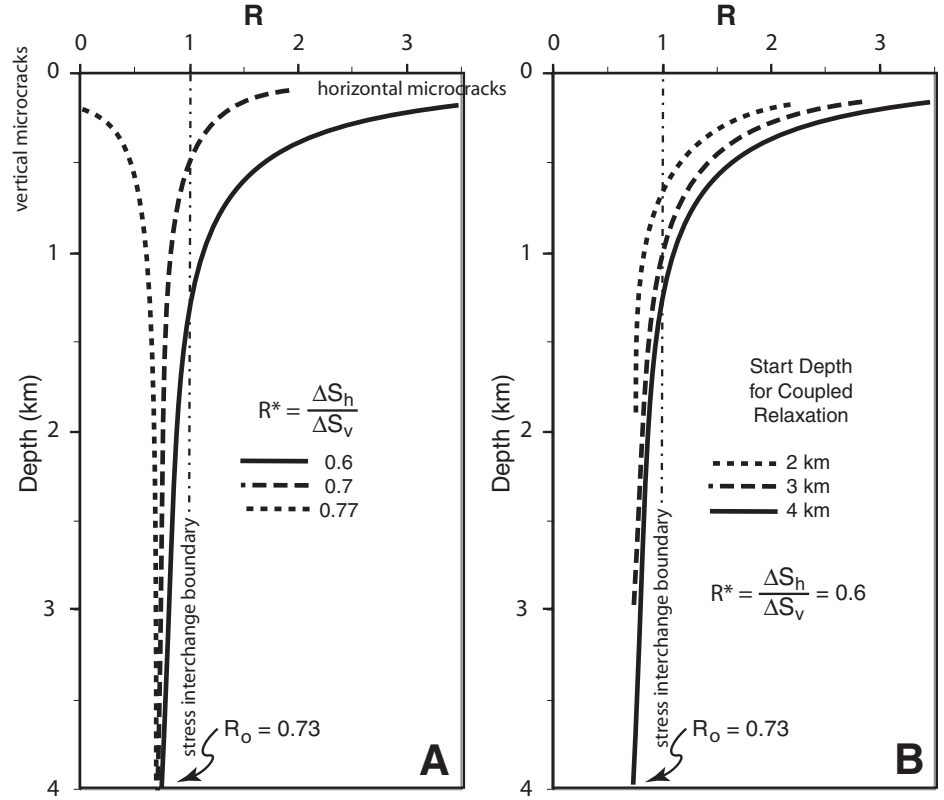


Figure 13. Hypothetical Brown-Hoek stress profiles for thermoelastic relaxation: (A) for three gradients, $\Delta S_{hmin}/\Delta z (= 0.6 \Delta S_v/\Delta z; = 0.7 \Delta S_v/\Delta z; = 0.77 \Delta S_v/\Delta z)$ starting at 4 km and $R = 0.73$. (B) Hypothetical Brown-Hoek stress profiles for thermoelastic relaxation starting at three depths (2 km, 3 km, 4 km) with $R = 0.73$ and $\Delta S_{hmin}/\Delta z = 0.6 \Delta S_v/\Delta z$.

tive of the BHSP, say $R_0 = (S_{hmin}/S_v)_0 = 0.73$ at some reference depth $z_0 = 4$ km. To do this, we calculate $R = f(z)$ according to

$$R = \frac{R_0 z_0 + R^* \Delta z}{z}, \quad (10)$$

where $S_{hmin}^0 = S_{hmin}$ and $S_v^0 = S_v$ at the reference depth z_0 , $\Delta S_{hmin} = S_{hmin} - S_{hmin}^0$, $\Delta S_v = S_v - S_v^0$, and $z =$ depth (Fig. 13). If R^* is a large fraction of the overburden gradient (e.g., 0.77 in Fig. 13A), tensile S_{hmin} (indicated by a negative R) will develop during exhumation at a depth of ~200 m, and there will be no interchange of vertical σ_2 and horizontal σ_3 , a situation inconsistent with the BHSP. $R^* < 0.7$ leads to an interchange of σ_2 and σ_3 (curves bending right in Fig. 13A) and a stress profile consistent with the BHSP. The depth of the stress interchange is found where the curves of Figure 13 cross $R = 1$. For smaller values of R^* starting at $R_0 = 0.73$, a deeper onset of relaxation yields a larger R in the near surface and a deeper interchange of vertical σ_2 and horizontal σ_3 (Fig. 13B). When $R^* < 0.6$, S_{hmin} in the upper km becomes large, however, topographic factors would come into play to limit the values

of S_{hmin} near the surface (Martel, 2006). In summary, values of R^* in the range of 0.6–0.7 yield R -curves that best match the BHSP.

Now that we understand the range of R^* that yields the characteristics of a thermoelastic relaxation consistent with the BHSP, we return to Equation 9 to consider the effect of rock properties on R^* . These calculations do not include the addition of a tectonic stress. Three rock properties, α , ν , E , and the geothermal gradient $\Delta T/\Delta z$ all affect R^*

$$R^* = \frac{\alpha_r E (\Delta T/\Delta z) + \nu \rho_c g + E (\rho_c/\rho_m) 1/a}{(1-\nu) \rho_c g} \quad (11)$$

with each parameter having a different effect (Fig. 14). Young's modulus, E , of granite and granodiorite falls in a range between 16 and 70 GPa (Haas, 1989). Preliminary calculations show that if $E = 70$ GPa for granite during exhumation along normal continental geotherms, $R^* > 0.7$, regardless of ν . The stiffest granite would enter the tensile field and fail by vertical jointing

rather than follow BHSP into the uppermost crust. To generate the BHSP on a geothermal gradient near 20 °C/km, the granite body must have an E on the order of 40 GPa, $\alpha = 0.000008$ °C⁻¹ and $0.1 < \nu < 0.15$. These are representative properties for granite (Haas, 1989). For geothermal gradients >25 °C/km, relaxation must start at a much shallower depths to yield the BHSP.

The effect of introducing cracks into granite is to reduce both the stiffness of the rock and thermal expansivity (O'Connell and Budiansky, 1974). A reduction in either of these parameters tends to shift the permissible range of R^* to higher geothermal gradients for the same range of Poisson's ratio (Fig. 14). Introducing cracks is one mechanism for buffering stress in the compressive field and, in this regard, the results given here are similar to those of Bruner (1984).

The data compilation leading to the BHSP paradigm shows interchange of σ_2 and σ_3 at very shallow depths in some instances (Fig. 1). Likewise, our calculations show that the evolution of the BHSP is sensitive to rock properties and the geothermal gradient. Given these observations, it is not surprising that rift planes are sometimes vertical as is the case for the Barre granite, which may reflect an $R^* > 0.7$ (Fig. 13). The formation of vertical neotectonic joints also reflects a relatively large R^* during the exhumation of sedimentary basins (e.g., Hancock and Engelder, 1989).

Near-Surface Structures and Earthquakes

Intracontinental crust carries a horizontal compression that persists to surface bedrock. Of course, the principal stresses are magnified and tilted by topography that is responsible for sheet fracturing (Miller and Dunne, 1996; Martel, 2006). Horizontal compression is responsible for other structures including bornhardts (Twidale and Bourne, 1998), A-tents (or pop-ups) (Ericson and Olvmo, 2004), and displaced slabs (Twidale and Bourne, 2000). It may also be a mechanism for effectively breaking bedrock apart and feeding it into the C-horizon of soil. Some data suggest that "microcracks commonly parallel sheets even where the sheets are steeply inclined" (Holzhausen, 1989). The data in the present paper suggest that while horizontal sheet fracturing is parallel to horizontal microcracks in the case of the Mason quarry (Fig. 3), such parallelism is not a universal rule as seen at the Kittredge quarry (Fig. 9).

The question about the timing of sheet fracturing relative to horizontal microcrack propagation persists. Horizontal to subhorizontal microcracking is pervasive and does not seem to follow topography in the same manner as sheet fracturing. Macroscopic tension is developed

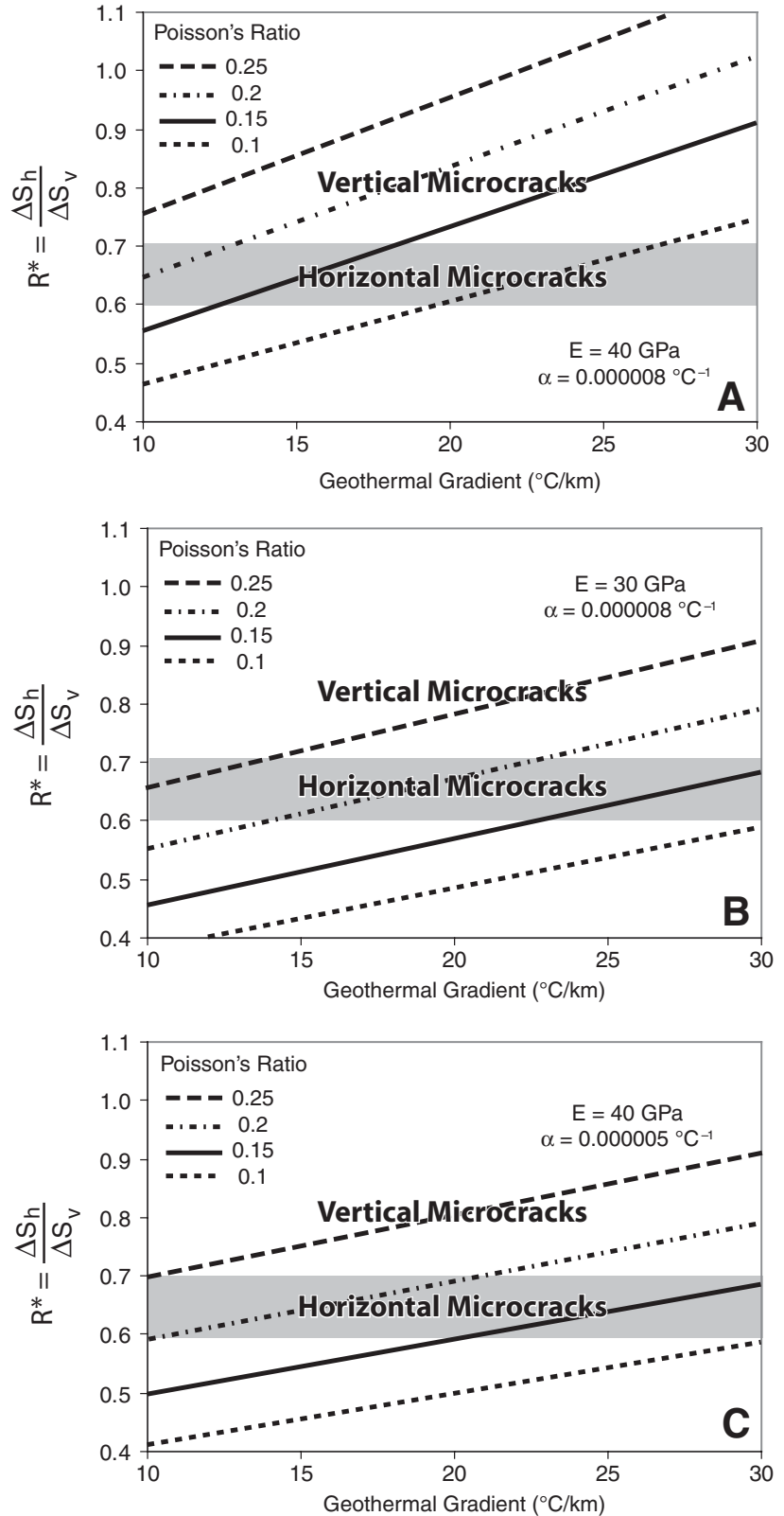


Figure 14. Normalized rate of thermoelastic relaxation, $R^* = \Delta S_{hmin} / \Delta S_v$, as a function of geothermal gradient in an upper crust for a granite with various effective Poisson's ratios, ν . (A) $E = 40$ MPa, $\alpha = 0.000008$ °C⁻¹; (B) $E = 30$ MPa, $\alpha = 0.000008$ °C⁻¹; (C) $E = 40$ MPa, $\alpha = 0.000005$ °C⁻¹. The horizontal shading defines the range of R^* that produces a BHSP consistent with Figure 1. Fields favoring horizontal and vertical microcracking are indicated.

by topography and relieved by sheet fracturing. Microcracking is a manifestation of microscopic tension that may develop even in the presence of a small but vertical compressive stress. Although we invoke the “Brazil test mechanism” for microcrack growth amounting to a couple of grain diameters long, the length of the macroscopic joints suggests that they propagated in an environment of absolute tension by the type presented by topographic perturbations (Miller and Dunne, 1996; Martel, 2006). In this scenario, horizontal microcracking is a deeper phenomenon in the upper crust than sheet fracturing.

If the remnant stress mechanism operates globally, particularly in intracontinental settings as indicated by the BHSP, it might affect the distribution of earthquakes in the upper crust (<2 km). Certainly, in the World Stress Map database for the USA east of longitude 104°W, this is the case, with 90% of the mechanisms reflection thrust or thrust-strike slip earthquakes for events of 2 km or less (Fig. 1). The Canadian data set is not as clear in this matter, although the two earthquakes <2 km are thrust mechanisms. This observation is, however, at odds with a California data set showing both P and T axes in the horizontal plane in the top 1.5 km of the crust (Bokelmann and Beroza, 2000).

CONCLUSIONS

Microcracks in granite develop in response to thermoelastic relaxation. Isobaric cooling leads to the early growth of vertical FIP but only after the granite has cooled on the order of 200 °C below the solidus. The driving stress for microcracking is a microscopic horizontal tension developed in response to a vertical load acting through grains that are nearly unconfined by isobaric cooling. Later exhumation leads to a relaxation of horizontal compressive stresses driven by the superposition of isobaric cooling and isothermal decompression at depths <4 km along a continental geotherm where $\Delta S_{hmin}/\Delta S_v < 1$ so that the state of stress becomes $S_{Hmax} > S_{hmin} \gg S_v$ in the near surface. The interchange of σ_2 and σ_3 leading to the BHSP takes place as long as the Young's modulus of the granite is on the order of 30–40 GPa. A stress state of $S_{Hmax} > S_{hmin} \gg S_v$ is consistent with the growth of late-stage horizontal microcracks. Our analysis leads to the conclusion that tectonic stresses are not responsible for the interchange of σ_2 and σ_3 in the upper crust. If tectonic stress is present in the near surface as is suggested by $S_{Hmax} > S_{hmin}$, it is a remnant stress carried to the surface during exhumation. Otherwise, tectonic stress would go to zero in the near surface as suggested by Zoback (2007). Thermoelastic relaxation leads to a remnant stress and the BHSP that is consistent with the depth

distribution of earthquake focal mechanisms from the stable platform of the USA portion of North America. Finally, the BHSP is characteristic of the upper crust because the two components of exhumation-related horizontal stress that Turcotte and Schubert (2002) call the “thermal effect” and the “elastic effect [as a consequence of erosion]” are, in detail, not comparable.

ACKNOWLEDGMENTS

This project was supported by National Science Foundation grant EAR-04-40233. The management of Fletcher Granite Company, Rock of Ages Corporation, and Swenson Granite Company are thanked for issuing the permits that allowed sampling within their quarries. Mark Lespinasse, Don Fisher, and Chris Marone are thanked for reviewing early versions of this paper. We are particularly grateful to Steve Martel and Peter Eichhubl, both of whom gave so generously of their time and ideas in reviewing the submission version of this paper.

REFERENCES CITED

- Adams, J., 1982, Stress-relief buckles in the McFarland quarry, Ottawa: Canadian Journal of Earth Sciences, v. 19, p. 1883–1887.
- Adams, J., 1989, Postglacial faulting in Eastern Canada: Nature, origin and seismic hazard implications: Tectonophysics, v. 163, p. 323–331, doi: 10.1016/0040-1951(89)90267-9.
- Bergbauer, S., and Martel, S.J., 1999, Formation of joints in cooling plutons: Journal of Structural Geology, v. 21, p. 821–825, doi: 10.1016/S0191-8141(99)00082-6.
- Birch, F., 1966, Compressibility: Elastic constants, in Clark, S.P., Jr., Handbook of physical constants: Geological Society of America Memoir 97, p. 97–173.
- Bokelmann, G.H.R., and Beroza, G.C., 2000, Depth-dependent earthquake focal mechanism orientation: Evidence for a weak zone in the lower crust: Journal of Geophysical Research, v. 105, p. 21,683–21,695, doi: 10.1029/2000JB900205.
- Brace, W.F., and Kohlstedt, D.L., 1980, Limits on lithospheric stress imposed by laboratory experiments: Journal of Geophysical Research, v. 85, p. 6248–6252, doi: 10.1029/JB085iB11p06248.
- Brace, W.F., Paulding, B., and Scholz, C.H., 1966, Dilatancy in the fracture of crystalline rocks: Journal of Geophysical Research, v. 71, p. 3939–3954.
- Bradley, D.C., Tucker, R.D., Lux, D.R., Harris, A.G., and McGregor, D.C., 2000, Migration of the Acadian Orogen and Foreland Basin across the northern Appalachians of Maine and adjacent areas: U.S. Geological Survey Professional Paper 1624, 49 p.
- Brown, E.T., and Hoek, E., 1978, Trends in relationships between measured in situ stresses and depth: International Journal of Rock Mechanics and Mining Sciences and Geomechanics Abstracts, v. 15, p. 211–215, doi: 10.1016/0148-9062(78)91227-5.
- Brudy, M., Zoback, M.D., Fuchs, K., Rummel, F., and Baumgartner, J., 1997, Estimation of the complete stress tensor to 8 km depth in the KTB scientific drill holes: Implications for crustal strength: Journal of Geophysical Research, v. 102, p. 18,453–18,475, doi: 10.1029/96JB02942.
- Bruner, W.M., 1979, Crack growth and the thermoelastic behavior of rocks: Journal of Geophysical Research, v. 84, p. 5578–5590, doi: 10.1029/JB084iB10p05578.
- Bruner, W.M., 1984, Crack growth during unroofing of crustal rocks: Effects on thermoelastic behavior and near-surface stresses: Journal of Geophysical Research, v. 89, p. 4167–4184, doi: 10.1029/JB089iB06p04167.
- Byerlee, J., 1978, Friction in rocks: Pure and Applied Geophysics, v. 116, p. 615–626, doi: 10.1007/BF00876528.
- Carlson, S.R., and Wang, H.F., 1986, Microcrack porosity and in situ stress in Illinois borehole UPH 3: Journal

- of Geophysical Research, v. 91, p. 10,421–10,428, doi: 10.1029/JB091iB10p10421.
- Chen, Y., Nishiyama, T., Kusuda, H., Kita, H., and Sato, T., 1999, Correlation between microcrack distribution patterns and granitic rock splitting planes: International Journal of Rock Mechanics and Mining Sciences, v. 36, p. 535–541, doi: 10.1016/S0148-9062(99)00014-5.
- Coates, D.F., 1964, Residual stress in rocks, in Judd, W.R., ed., State of stress in the Earth's crust: Proceedings of the International Conference, 1–14 June 1963, Santa Monica, California: New York, Elsevier, p. 679–688.
- Dale, T.N., 1923, The commercial granites of New England: U.S. Geological Survey Bulletin 738, 488 p.
- DeGraft, J.M., and Aydin, A., 1987, Surface morphology of columnar joints and its significance to mechanics and direction of joint growth: Geological Society of America Bulletin, v. 99, p. 605–617, doi: 10.1130/0016-7606(1987)99<605:SMOCSA>2.0.CO;2.
- Dezayes, C., Villemain, T., and Pêcher, A., 2000, Microfracture pattern compared to core-scale fractures in the borehole of soultz-sous-Forêts granite, Rhine graben, France: Journal of Structural Geology, v. 22, p. 723–733, doi: 10.1016/S0191-8141(00)00003-1.
- Douglass, P.M., and Voight, B., 1969, Anisotropy of granites—A reflection of microscopic fabric: Geotechnique, v. 19, p. 376–398.
- Durucan, S., Korre, A., and Diehl, M., 2000, Classification of micro-geoparametric parting planes in granites: International Journal of Surface Mining, Reclamation, and Environment, v. 14, p. 103–119, doi: 10.1080/13895260008953307.
- Eberhardt, E., Stead, D., and Stimpson, B., 1999, Quantifying progressive pre-peak brittle fracture damage in rock during uniaxial compression: International Journal of Rock Mechanics and Mining Sciences, v. 36, p. 361–380, doi: 10.1016/S0148-9062(99)00019-4.
- Engelder, T., 1984, The time-dependent strain relaxation of Algeria granite: International Journal of Rock Mechanics and Mining Sciences and Geomechanics Abstracts, v. 21, p. 63–73, doi: 10.1016/0148-9062(84)91174-4.
- Engelder, T., 1993, Stress regimes in the lithosphere: Princeton, New Jersey, Princeton Press, 451 p.
- Ericson, K., and Olvmo, M., 2004, A-tents in the central Sierra Nevada, California: A geomorphological indicator of tectonic stress: Physical Geography, v. 25, p. 291–312, doi: 10.2747/0272-3646.25.4.291.
- Fleischmann, K.H., 1990, Rift and grain in two New England granites: Journal of Geophysical Research, v. 95, p. 21,463–21,474, doi: 10.1029/JB095iB13p21463.
- Friedman, M., 1972, Residual elastic strain in rocks: Tectonophysics, v. 15, p. 297–330, doi: 10.1016/0040-1951(72)90093-5.
- Friedman, M., and Bur, T.R., 1974, Investigation of the relations among residual strain, fabric, fracture and ultrasonic attenuation and velocity in rocks: International Journal of Rock Mechanics and Mining Sciences and Geomechanics Abstracts, v. 11, p. 221–234, doi: 10.1016/0148-9062(74)90129-6.
- Haas, C.J., 1989, Static stress-strain relationships, in Touloukian, Y.S., Judd, W.R., and Roy, R.F., eds., Physical properties of rocks and minerals: CINDAS Data Series on Material Properties, v. II-2, p. 123–176.
- Haimson, B.C., and Doe, T.W., 1983, State of stress, permeability, and fractures in the Precambrian granite of northern Illinois: Journal of Geophysical Research, v. 88, p. 7355–7372, doi: 10.1029/JB088iB09p07355.
- Hancock, P.L., and Engelder, T., 1989, Neotectonic joints: Geological Society of America Bulletin, v. 101, p. 1197–1208, doi: 10.1130/0016-7606(1989)101<1197: NJ>2.3.CO;2.
- Harper, T.R., Appel, G., Pendleton, M.W., Szmanski, J.S., and Taylor, R.K., 1979, Swelling strain development in sedimentary rocks in northern New York: International Journal of Rock Mechanics and Mining Sciences and Geomechanics Abstracts, v. 16, p. 271–292, doi: 10.1016/0148-9062(79)90239-0.
- Haxby, W.F., and Turcotte, D.L., 1976, Stresses induced by the addition or removal of overburden and associated thermal effects: Geology, v. 4, p. 181–184, doi: 10.1130/0091-7613(1976)4<181:SBTAO>2.0.CO;2.
- Hazzard, J.F., Young, R.P., and Maxwell, S.C., 2000, Micromechanical modeling of cracking and failure in

- brittle rocks: *Journal of Geophysical Research*, v. 105, p. 16,683–16,697, doi: 10.1029/2000JB900085.
- Herget, G., 1993, Rock stresses and rock stress monitoring in Canada, in Hudson, J.A., ed., *Rock testing and site characterization: Comprehensive rock engineering*: Oxford, Pergamon Press, p. 473–496.
- Holzhausen, G.R., 1989, Origin of sheet structures, 1, Morphology and boundary conditions: *Engineering Geology*, v. 27, p. 225–278, doi: 10.1016/0013-7952(89)90035-5.
- Hondros, G., 1959, The evaluation of Poisson's ratio and the modulus of materials of low tensile resistance by the Brazilian (indirect tensile) test with particular reference to concrete: *Australian Journal of Applied Science*, v. 10, p. 243–268.
- Hooker, V.E., and Johnson, C.F., 1969, Near-surface horizontal stresses, including the effects of rock anisotropy: Washington, D.C., Report of Investigations 7224, U.S. Bureau of Mines, 29 p.
- Jahns, R.H., 1943, Sheet structure in granites: Its origin and use as a measure of glacial erosion in New England: *The Journal of Geology*, v. 51, p. 71–98.
- Jang, B.-A., and Wang, H.F., 1991, Micromechanical modeling of healed crack orientations as a paleostress indicator: Application to Precambrian granite from Illinois and Wisconsin: *Journal of Geophysical Research*, v. 96, p. 19,655–19,664, doi: 10.1029/91JB01938.
- Johnson, A.M., 1970, Physical processes in geology: New York, Freeman, Cooper and Company, 577 p.
- Karig, D.E., and Hou, G., 1992, High-stress consolidation experiments and their geological implications: *Journal of Geophysical Research*, v. 97, p. 289–300, doi: 10.1029/91JB02247.
- Kowallis, B.J., Wang, H.F., and Jang, B.A., 1987, Healed microcrack orientations in granite from Illinois borehole UPH-3 and their relationship to the rocks stress history: *Tectonophysics*, v. 135, p. 297–306, doi: 10.1016/0040-1951(87)90114-4.
- Kranz, R.L., 1983, Microcracks in review: *Tectonophysics*, v. 100, p. 449–480, doi: 10.1016/0040-1951(83)90198-1.
- Laubach, S.E., 1989, Paleostress directions from the preferred orientation of closed microfractures (fluid-inclusion planes) in sandstone, East Texas basin, U.S.A.: *Journal of Structural Geology*, v. 11, p. 603–612, doi: 10.1016/0191-8141(89)90091-6.
- Lawn, B., 1993, *Fracture of brittle solids*: Second edition: Cambridge, Cambridge University Press, 378 p.
- Lespinasse, M., and Pecher, A., 1986, Microfracturing and regional stress field: A study of the preferred orientations of fluid inclusion planes in a granite from the Massif Central, France: *Journal of Structural Geology*, v. 8, p. 169–180, doi: 10.1016/0191-8141(86)90107-0.
- Lespinasse, M., Désindes, L., Frateczak, P., and Petrov, V., 2005, Microfissural mapping of natural cracks in rocks: Implications for fluid transfers quantification in the crust: *Chemical Geology*, v. 223, p. 170–178, doi: 10.1016/j.chemgeo.2005.05.009.
- Lund, B., and Zoback, M.D., 1999, Orientation and magnitude of in situ stress to 6.5 km depth in the Baltic Shield: *International Journal of Rock Mechanics and Mining Sciences*, v. 36, p. 169–190, doi: 10.1016/S0148-9062(98)00183-1.
- Martel, S.J., 2006, Effect of topographic curvature on near-surface stresses and application to sheeting joints: *Geophysical Research Letters*, v. 33, L01208, 5 p.
- Martin, R.J., 1972, Time-dependent crack growth in quartz and its application to the creep of rocks: *Journal of Geophysical Research*, v. 77, p. 1406–1419, doi: 10.1029/JB077i008p01406.
- McGarr, A., and Gay, N.C., 1978, State of stress in the Earth's crust: *Annual Review of Earth and Planetary Sciences*, v. 6, p. 405–436, doi: 10.1146/annurev.ea.06.050178.002201.
- Miller, D.J., and Dunne, T., 1996, Topographic perturbations of regional stresses and consequent bedrock fracturing: *Journal of Geophysical Research*, v. 101, p. 25,523–25,536, doi: 10.1029/96JB02531.
- Narr, W., and Currie, J.B., 1982, Origin of fracture porosity—Example from Altamont field, Utah: *American Association of Petroleum Geologists Bulletin*, v. 66, p. 1231–1247.
- Nasser, M.H.B., Mohanty, B., and Robin, P.-Y.F., 2005, Characterization of microstructures and fracture toughness in five granitic rocks: *International Journal of Rock Mechanics and Mining Sciences*, v. 42, p. 450–460, doi: 10.1016/j.ijrmms.2004.11.007.
- Nur, A., and Simmons, G., 1970, The origin of small cracks in igneous rocks: *International Journal of Rock Mechanics and Mining Sciences and Geomechanics Abstracts*, v. 7, p. 307–314, doi: 10.1016/0148-9062(70)90044-6.
- O'Connell, R.J., and Budiansky, B., 1974, Seismic velocities in dry and saturated cracked solids: *Journal of Geophysical Research*, v. 79, p. 5412–5426, doi: 10.1029/JB079i035p05412.
- Olson, J.E., and Pollard, D.D., 1989, Inferring paleostress from natural fracture patterns: A new method: *Geology*, v. 17, p. 345–348, doi: 10.1130/0091-7613(1989)017<0345:IPFNFP>2.3.CO;2.
- Osborne, F.F., 1935, Rift, grain, and hardway in some Precambrian granites, Quebec: *Economic Geology and the Bulletin of the Society of Economic Geologists*, v. 30, p. 540–551.
- Pecher, A., Lespinasse, M., and Leroy, J., 1985, Relations between fluid inclusion trails and regional stress field: A tool for fluid chronology—An example of an intragranitic uranium ore deposit (northwest Massif Central, France): *Lithos*, v. 18, p. 229–237, doi: 10.1016/0024-4937(85)90027-1.
- Plumb, R.A., 1994, Variations of the least horizontal stress magnitude in sedimentary rocks, in Nelson, P.P., and Laubach, S.E., eds., *Rock mechanics models and measurements: Challenges from industry*: Rotterdam, Netherlands, A.A. Balkema, p. 71–78.
- Plumb, R.A., Engelder, T., and Yale, D., 1984, Near surface in situ stress, 3. Correlation with microcrack fabric within the New Hampshire granites: *Journal of Geophysical Research*, v. 89, p. 9350–9364, doi: 10.1029/JB089iB11p09350.
- Pollard, D.D., and Aydin, A., 1988, Progress in understanding jointing over the past century: *Geological Society of America Bulletin*, v. 100, p. 1181–1204, doi: 10.1130/0016-7606(1988)100<1181:PIUJOT>2.3.CO;2.
- Pollard, D.D., and Segall, P., 1987, Theoretical displacements and stresses near fractures in rock: With applications to faults, joints, veins, dikes, and solution surfaces, in Atkinson, B., ed., *Fracture mechanics of rock*: Orlando, Academic Press, p.227–350.
- Price, N.J., 1966, *Fault and joint development in brittle and semi-brittle rock*: London, Pergamon Press, 176 p.
- Price, N.J., 1979, Fracture patterns and stresses in granites: *Geoscience Canada*, v. 6, p. 209–212.
- Ranalli, G., and Chandler, T.E., 1975, The stress field in the upper crust as determined from in situ measurements: *Geologische Rundschau*, v. 64, p. 653–674, doi: 10.1007/BF01820688.
- Robinson, P., Tucker, R.D., Bradley, D., Berry, H.N., IV, and Osberg, P.H., 1998, Paleozoic orogens in New England, USA: *Geologiska Föreningens i Stockholm Förhandlingar (GFF)*, v. 120, p. 119–148.
- Savage, W.Z., 1978, The development of residual stress in cooling rock bodies: *Geophysical Research Letters*, v. 5, p. 633–636, doi: 10.1029/GL005i008p0633.
- Sbar, M.L., Richardson, R.M., Flaccus, C., and Engelder, T., 1984, Near-surface in situ stress: 1. Strain relaxation measurements along the San Andreas fault in southern California: *Journal of Geophysical Research*, v. 89, p. 9323–9332, doi: 10.1029/JB089iB11p09323.
- Skinner, B.J., 1966, Thermal expansion, in Clark, S.P., Jr., *Handbook of physical constants*: Geological Society of America Memoir 97, p. 75–96.
- Smith, D. L. and Evans, B., 1984, Diffusional crack healing in quartz: *Journal of Geophysical Research*, v. 89, p. 4125–4135.
- Szczepanik, Z., Milne, D., Kostakis, K., and Eberhardt, E., 2003, Long term laboratory strength tests in hard rock, in Handley, M., and Stacey, D., *Technology roadmap for rock mechanics*: Johannesburg, Tenth Congress of the International Society for Rock Mechanics, South African Institute of Mining and Metallurgy, p. 1179–1184.
- Takemura, T., Golshani, A., Oda, M., and Suzuki, K., 2003, Preferred orientations of open microcracks in granite and their relation with anisotropic elasticity: *International Journal of Rock Mechanics and Mining Sciences*, v. 40, p. 443–454, doi: 10.1016/S1365-1609(03)00014-5.
- Takeshita, T., and Yagi, K., 2001, Paleostress orientation from 3-D orientation distribution of microcracks in quartz from the Cretaceous granodiorite core samples drilled through the Nojima Fault, south-west Japan: *The Island Arc*, v. 10, p. 495–505, doi: 10.1046/j.1440-1738.2001.00348.x.
- Turcotte, D.L., and Schubert, G., 2002, *Geodynamics—Second Edition*: Cambridge, Cambridge University Press, 456 p.
- Tuttle, O.F., 1949, Structural petrology of planes of liquid inclusions: *The Journal of Geology*, v. 57, p. 331–356.
- Twidale, C.R., and Bourne, J.A., 1998, Origin and age of bornhardts, southwest Western Australia: *Australian Journal of Earth Sciences*, v. 45, p. 903–914, doi: 10.1080/08120099808728444.
- Twidale, C.R., and Bourne, J.A., 2000, Rock bursts and associated neotectonic forms at Minnipa Hill, northwestern Eyre Peninsula, South Australia: *Environmental and Engineering Geoscience*, v. 6, p. 129–140.
- Varnes, D.J., and Lee, F.T., 1972, Hypothesis of mobilization of residual stress in rock: *Geological Society of America Bulletin*, v. 83, p. 2863–2866, doi: 10.1130/016-7606(1972)83[2863:HOMORS]2.0.CO;2.
- Voight, B., 1966, Beziehung zwischen grossen horizontalen Spannungen im Begirge und der Tektonik und der Abtragung: *Proceedings of the 1st Congress of International Society of Rock Mechanics*, v. 2, p. 51–56.
- Voight, B., 1974, A mechanism for “locking-in” orogenic stress: *American Journal of Science*, v. 274, p. 662–665.
- Voight, B., and St. Pierre, B.H.P., 1974, Stress history and rock stress: *Advances in rock mechanics: Proceedings Third Congress International Society of Rock Mechanics*, v. 2, p. 580–582.
- Vollbrecht, A., Rust, S., and Weber, K., 1991, Development of microcracks in granites during cooling and uplift: Examples from the Variscan basement of NE Bavaria, Germany: *Journal of Structural Geology*, v. 13, p. 787–799, doi: 10.1016/0191-8141(91)90004-3.
- Wang, Q.Z., Jia, X.M., Kou, S.Q., Zhang, Z.X., and Lindqvist, P.A., 2004, The flattened Brazilian disc specimen used for testing elastic modulus, tensile strength and fracture toughness of brittle rocks: Analytical and numerical results: *International Journal of Rock Mechanics and Mining Sciences*, v. 41, p. 245–253, doi: 10.1016/S1365-1609(03)00093-5.
- Wilson, J.E., Chester, J.S., and Chester, F.M., 2003, Microfracture analysis of fault growth and wear process, Punchbowl Fault, San Andreas system, California: *Journal of Structural Geology*, v. 25, p. 1855–1873, doi: 10.1016/S0191-8141(03)00036-1.
- Winslow, D.M., Bodnar, R.J., and Tracy, R.J., 1994, Fluid inclusion evidence for an anticlockwise metamorphic P-T path in central Massachusetts: *Journal of Metamorphic Geology*, v. 12, p. 361–371, doi: 10.1111/j.1525-1314.1994.tb00029.x.
- Wise, D.U., 1964, Microjointing in basement, Middle Rocky Mountains of Montana and Wyoming: *Geological Society of America Bulletin*, v. 75, p. 287–306, doi: 10.1130/0016-7606(1964)75[287:MIBMRM]2.0.CO;2.
- Wise, D.U., 2005, Rift and grain in basement: Thermally triggered snapshots of stress fields during erosional unroofing of the Rocky Mountains of Montana and Wyoming: *Rocky Mountain Geology*, v. 40, p. 193–209, doi: 10.2113/40.2.193.
- Wong, T.F., 1982, Micromechanics of faulting in Westerly granite: *International Journal of Rock Mechanics and Mining Sciences and Geomechanics Abstracts*, v. 19, p. 49–64, doi: 10.1016/0148-9062(82)91631-X.
- Zoback, M.D., and Townend, J., 2001, Implications of hydrostatic pore pressures and high crustal strength for the deformation of intraplate lithosphere: *Tectonophysics*, v. 336, p. 19–30, doi: 10.1016/S0040-1951(01)00091-9.
- Zoback, M.D., 2007, *Reservoir geomechanics*: Cambridge, Cambridge University Press, 449 p.

MANUSCRIPT RECEIVED 14 FEBRUARY 2007
 REVISED MANUSCRIPT RECEIVED 10 JANUARY 2008
 MANUSCRIPT ACCEPTED 15 JANUARY 2008

Printed in the USA